Short Article

Cell Host & Microbe

A *Listeria monocytogenes* Bacteriocin Can Target the Commensal *Prevotella copri* and Modulate Intestinal Infection

Graphical Abstract

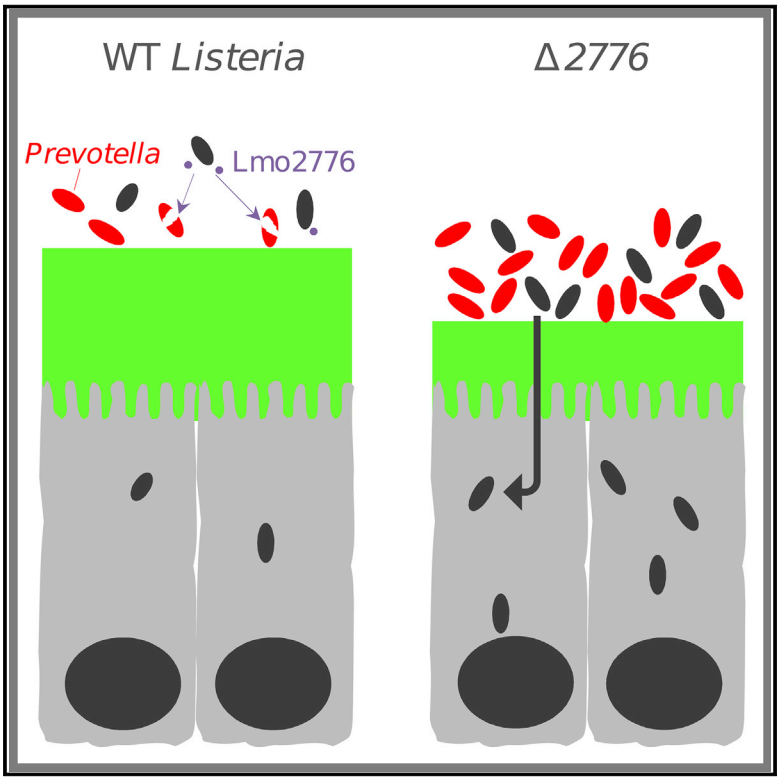

Authors

Nathalie Rolhion, Benoit Chassaing, Marie-Anne Nahori, ..., Andrew T. Gewirtz, Tom Van de Wiele, Pascale Cossart

Correspondence

pascale.cossart@pasteur.fr

In Brief

While studying the impact of a previously unknown *Listeria monocytogenes* bacteriocin on infection, Rolhion et al. identify *P. copri*, an abundant gut commensal, as the primary target of this bacteriocin in the gut microbiota and as a modulator of infection.

Highlights

- *L. monocytogenes* secretes a bacteriocin (Lmo2776) homologous to the lactococcin 972
- Lmo2776 controls *Listeria* intestinal colonization in a microbiota-dependent manner
- Lmo2776 targets the abundant gut commensal *Prevotella copri*
- Presence of *P. copri* exacerbates infection

Rolhion et al., 2019, Cell Host & Microbe *26*, 691–701
November 13, 2019
https://doi.org/10.1016/j.chom.2019.10.016

CellPress

Cell Host & Microbe
Short Article

A *Listeria monocytogenes* Bacteriocin Can Target the Commensal *Prevotella copri* and Modulate Intestinal Infection

Nathalie Rolhion,[1,2,3,14] Benoit Chassaing,[4,5,15] Marie-Anne Nahori,[1,2,3] Jana de Bodt,[6] Alexandra Moura,[7,8] Marc Lecuit,[7,8,9] Olivier Dussurget,[1,2,3,10] Marion Bérard,[11] Massimo Marzorati,[6] Hannah Fehlner-Peach,[12] Dan R. Littman,[12,13] Andrew T. Gewirtz,[5,16] Tom Van de Wiele,[6,16] and Pascale Cossart[1,2,3,17,*]

[1]Institut Pasteur, Unité des Interactions Bactéries-Cellules, 75015 Paris, France
[2]Inserm, U604, 75015 Paris, France
[3]INRA, Unité sous-contrat 2020, 75015 Paris, France
[4]Neurosciences Institute, Georgia State University (GSU), Atlanta, GA 30303, USA
[5]Center for Inflammation, Immunity and Infection, Institute for Biomedical Sciences, GSU, Atlanta, GA 30303, USA
[6]Center of Microbial Ecology and Technology, Faculty of Bioscience Engineering, Ghent University, 9000 Ghent, Belgium
[7]Institut Pasteur, Unité Biologie des Infections, 75015 Paris, France
[8]Inserm, U1117, 75015 Paris, France
[9]Paris Descartes University, Sorbonne Paris Cité, Division of Infectious Diseases and Tropical Medicine, Necker-Enfants Malades University Hospital, Institut Imagine, 75743 Paris, France
[10]Université de Paris, 75013 Paris, France
[11]Animalerie Centrale, Department of Technology and Scientific Programmes, Institut Pasteur, 75015 Paris, France
[12]The Kimmel Center for Biology and Medicine of the Skirball Institute, New York University School of Medicine, New York, NY 10016, USA
[13]Howard Hughes Medical Institute, New York, NY 10016, USA
[14]Present address: Microbiote, Intestin et Inflammation, Inserm, UMRS-938, Centre de Recherche Saint-Antoine, 75012 Paris, France
[15]Present address: Mucosal Microbiota in Chronic Inflammatory Diseases, INSERM, 75014 Paris
[16]These authors contributed equally
[17]Lead Contact
*Correspondence: pascale.cossart@pasteur.fr
https://doi.org/10.1016/j.chom.2019.10.016

SUMMARY

Understanding the role of the microbiota components in either preventing or favoring enteric infections is critical. Here, we report the discovery of a *Listeria* bacteriocin, Lmo2776, which limits *Listeria* intestinal colonization. Oral infection of conventional mice with a Δ*lmo2776* mutant leads to a thinner intestinal mucus layer and higher *Listeria* loads both in the intestinal content and deeper tissues compared to WT *Listeria.* This latter difference is microbiota dependent, as it is not observed in germ-free mice. Strikingly, it is phenocopied by pre-colonization of germ-free mice before *Listeria* infection with *Prevotella copri*, an abundant gut-commensal bacteria, but not with the other commensals tested. We further show that Lmo2776 targets *P. copri* and reduces its abundance. Together, these data unveil a role for *P.copri* in exacerbating intestinal infection, highlighting that pathogens such as *Listeria* may selectively deplete microbiota bacterial species to avoid excessive inflammation.

INTRODUCTION

Prevotella is classically considered a common commensal bacterium due to its presence in several locations of the healthy human body, including the oral cavity, gastrointestinal tract, urogenital tract, and skin (Larsen, 2017). The *Prevotella* genus encompasses more than 40 different culturable species of which three—*P. copri* (*Pc*), *P. salivae* (*Ps*), and *P. stercorea*—are members of the gut microbiota. *Prevotella* has been reported to be associated with opportunistic infections, e.g., periodontitis or bacterial vaginosis (Larsen, 2017). Moreover, *Prevotella* is the major genus of one of the three reported human enterotypes (Arumugam et al., 2011), but how *Prevotella* behaves in different gut ecosystems and how it interacts with other bacteria of the microbiota and/or with its host is not well defined. In addition, high levels of genomic diversity within *Prevotella* strains of the same species have been observed (De Filippis et al., 2019; Gupta et al., 2015), which adds another layer of complexity for predicting the effects of *Prevotella* strains. Recent studies have linked higher intestinal abundance of *Pc* to rheumatoid arthritis (Alpizar-Rodriguez et al., 2019; Maeda et al., 2016; Scher et al., 2013), metabolic syndrome (Pedersen et al., 2016), low-grade systemic inflammation (Pedersen et al., 2016), and inflammation in the context of human immunodeficiency virus (HIV) infection (Dillon et al., 2016; Kaur et al., 2018; Lozupone et al., 2014), suggesting that some *Prevotella* strains may trigger and/or worsen inflammatory diseases (Larsen, 2017; Ley, 2016; Precup and Vodnar, 2019).

The microbiota plays a central role in protecting the host from pathogens, in part through colonization resistance (Buffie and Pamer, 2013). In the case of *Listeria monocytogenes* (*Lm*), the foodborne pathogen responsible for listeriosis, the intestinal microbiota provides protection, as germfree mice are more

susceptible to infection than conventional mice (Archambaud et al., 2013; Becattini et al., 2017). Treatment with probiotics such as *Lactobacillus paracasei* CNCM I-3689 or *L. casei* BL23 was shown to decrease *Lm* systemic dissemination in orally inoculated mice (Archambaud et al., 2012). Unravelling the interactions between the host, the microbiota, and pathogenic bacteria is critical for the design of new therapeutic strategies via manipulation of the microbiota. However, identifying specific molecules and mechanisms used by commensals to elicit their beneficial action is challenging due to the high complexity of the microbiome, together with technical issues in culturing many commensal species. In addition, cooperative interactions between commensal species are likely to be central to the functioning of the gut microbiota (Rakoff-Nahoum et al., 2016). So far, mechanism or molecules underlying the impact of commensals on the host or on the infection have been elucidated only for a few species. For example, (i) segmented filamentous bacteria were shown to coordinate maturation of T cell responses toward Th17 cell induction (Gaboriau-Routhiau et al., 2009; Ivanov et al., 2009), (ii) glycosphingolipids produced by the common intestinal symbiont *Bacteroides fragilis* have been found to regulate homeostasis of host intestinal natural killer T cells (An et al., 2014), (iii) a polysaccharide A also produced by *B. fragilis* induces and expands Il-10 producing CD4+ T cells (Mazmanian et al., 2005; Mazmanian et al., 2008; Round and Mazmanian, 2010), (iv) the microbial anti-inflammatory molecule secreted by *Faecalibacterium prausnitzii* impairs the nuclear-factor-κB pathway (Quévrain et al., 2016), (v) *Mucispirillum schaedleri* protects mice from *Salmonella*-induced colitis (Herp et al., 2019), and (vi) *Blautia producta* restores resistance against vancomycin-resistant enterococci (Kim et al., 2019).

Conversely, enteric pathogens evolved various means to outcompete other species in the intestine and access nutritional and spatial niches, leading to successful infection and transmission. In this regard, the contribution of bacteriocins and type VI secretion system effectors during pathogen colonization of the gut is an emerging field of investigation (Bäumler and Sperandio, 2016; Rolhion and Chassaing, 2016). Here, we studied the impact of a previous unknown *Lm* bacteriocin (Lmo2776) on infection, and we discovered that *Pc*, an abundant gut commensal, is the primary target of Lmo2776 in both the mouse and human microbiota and as a modulator of infection.

RESULTS

Lmo2776 Limits *Lm* Intestinal Colonization and Virulence in a Microbiota-Dependent Manner

A recent reannotation of the genome of the *Lm* strain EGD-e revealed that the *lmo2776* gene, absent in the non-pathogenic *L. innocua* species (Figure S1A), potentially encodes a secreted bacteriocin of 107 amino acids (Desvaux et al., 2010; Glaser et al., 2001), homologous to the lactococcin 972 (Lcn972) secreted by *Lactococcus lactis* (Martínez et al., 1996) and to putative bacteriocins of pathogenic bacteria *Streptococcus iniae* (Li et al., 2014), *Streptococcus pneumoniae*, and *Staphylococcus aureus* (Figure S1B). This gene belongs to a locus containing two other genes, *lmo2774* and *lmo2775,* encoding potential immunity and transport systems (Glaser et al., 2001). It is present in lineage I strains responsible for the majority of *Lm* clinical cases (Maury et al., 2016) and in some lineage II strains, such as EGD-e (Figure S1C). Little is known about this bacteriocin family, and studies have focused on Lcn972. Lmo2776 shares between 38% an d 47% overall amino acid sequence similarity with members of the Lcn972 family. Because expression of *lmo2774*, *lmo2775*, and *lmo2776* is significantly higher in stationary phase compared to exponential phase of EGD-e at 37°C in BHI (Figure S1D), all experiments described below were conducted with *Lm* grown up to stationary phase.

We first examined the effect of Lmo2776 on infection. We inoculated conventional BALB/c mice with either the WT, the Δ*lmo2776*, or the Lmo2776 complemented strains and compared *Lm* loads in the intestinal lumen and deeper organs (spleen and liver). We had verified that deletion of *lmo2776* was not affecting expression of surrounding genes, *lmo2774*, *lmo2775*, and *lmo2777* (Figure S1E) or bacterial growth *in vitro* (Figure S1F). Inoculation of mice with Δ*lmo2776* strain resulted in significantly higher *Lm* loads in the small intestinal lumen 24 h post-inoculation (pi) compared to the WT strain (Figure 1A). These differences persisted at 48 and 72 h pi (Figure S1G). *Lm* loads of Δ*lmo2776* were also significantly higher in the spleen and liver at 72 h pi compared to both WT and Lmo2776-complemented strains (Figures 1B and 1C). Similar results were observed in C57BL/6J mice (data not shown). Together, these results indicate a key role for Lmo2776 in bacterial colonization of intestine and deeper organs. Following intravenous inoculation of BALB/c mice with WT or Δ*lmo2776* bacteria, bacterial loads at 72 h pi were similar in the spleen and liver (Figure S1H), revealing that Lmo2776 exerts its primary role during the intestinal phase of infection and not later.

Considering that *lmo2776* is predicted to encode a bacteriocin and that it significantly affects the intestinal phase of infection, we hypothesized that Lmo2776 might target intestinal bacteria, thereby impacting *Lm* infection. To address the role of intestinal microbiota in infection, we orally inoculated germfree mice with WT or Δ*lmo2776* strains and compared bacterial counts 72 h pi. Strikingly, no significant difference was observed between WT and Δ*lmo2776* strains in the small intestinal content (Figure 1D) nor in spleen and liver (Figures 1E and 1F). These results showed that the Lmo2776 bacteriocin limits the presence in the deeper organs of WT *Lm* in a microbiota-dependent manner.

Lmo2776 Targets *Prevotella* in Mouse and Human Microbiota

To identify which intestinal bacteria were targeted by Lmo2776, we compared microbiota compositions of conventional mice orally infected with WT or Δ*lmo2776* strains by 16S rRNA gene sequencing. We first verified that the fecal microbiota composition of all mice was indistinguishable at day 0 (Figure 2A). As expected, the microbiota composition at day 1 pi was dramatically altered by infection with *Lm* WT (Figure S2A). These alterations in microbiota composition included reduced levels of *Bacteroidetes* phylum (relative abundance before infection: 65.4% and at day 1 pi: 42.4%) and increased levels of *Firmicutes* (relative abundance before infection: 29.9% and at day 1 pi: 54.0%) (Figure S2B–S2E). The increased levels in the *Firmicutes* were mainly due to an increase of the *Clostridia* class (relative abundance before infection: 27.4% and at day 1 pi: 50.7%). Of note, the relative abundance of *Lm* was around 0.1% and cannot therefore

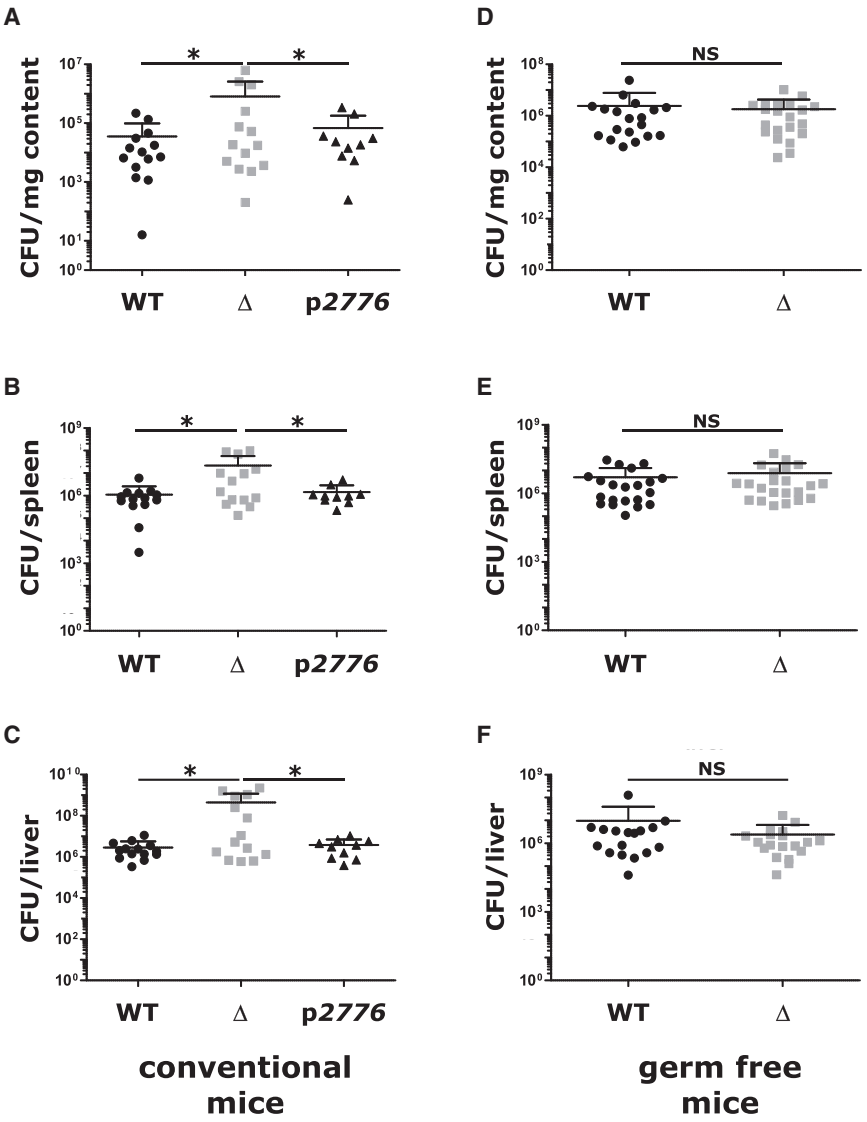

Figure 1. Lmo2776 Limits *Lm* Virulence in a Microbiota-Dependent Manner

(A–C) BALB/c mice were inoculated orally with *Lm* WT, Δ*lmo2776*, or Lmo2776 complemented (*p2776*) bacteria. CFUs in the intestinal luminal content (A), spleen (B), and liver (C) were assessed at 72 h pi.

(D–F) Germfree C57BL/6J were inoculated with *Lm* WT or Δ*lmo2776* for 72 h and CFUs in the intestinal luminal content (D), spleen (E), and liver (F) were assessed. Each dot represents the value for one mouse. Statistically significant differences were evaluated by the Mann–Whitney test (*p < 0.05; NS, not significant).

explain by itself the increased levels of *Firmicutes* observed between day 0 and day 1. Importantly, at 24 h and 48 h pi, intestinal microbial compositions differed in mice orally inoculated with Δ*lmo2776* strain compared to WT strain (Figure 2A). We focused on operational taxonomic units (OTUs) for which the relative abundance was identical before infection with *Lm* strains (day −3 to day 0) and was subsequently altered by at least a 2-fold difference at day 1 pi in mice infected with Δ*lmo2776* compared to mice infected with WT strain. In independent experiments, the relative abundance of 12 OTUs was lower in mice infected with WT strain compared to Δ*lmo2776* mutant (Figures 2B and 2C) at day 1 and also at day 2 pi. Phylogenetic analyses revealed that all these 12 OTUs belong to the *Prevotella* cluster (Figure 2D). A decrease of *Prevotella* in mice infected with WT strain at day 1 and day 2 pi compared to mice infected with Δ*lmo2776* strain was also observed by qPCR analysis using primers specific for *Prevotella* (Figure 2E).

Important differences exist between mouse and human gut microbiota composition. *Prevotella* abundance is known to be low in mouse intestinal content (< 1%), although it can reach 80% in human gut microbiota (Hildebrand et al., 2013; Nguyen et al., 2015). As *Lm* is a human pathogen, we searched to investigate the impact of Lmo2776 on human gut microbiota. For this purpose, we used a dynamic *in vitro* gut model (mucosal-simulator of human intestinal microbial ecosystem [M-SHIME]), which allows stable maintenance of human microbiota *in vitro* in absence of host cells but in presence of mucin-covered beads (Chassaing et al., 2017; Geirnaert et al., 2015; Van den Abbeele et al., 2013; Van den Abbeele et al., 2012) and therefore allows studies on human microbiota independently of the host responses (such as inflammation). The microbiota of a healthy human volunteer was inoculated to the system which was then infected with WT or Δ*lmo2776 Lm*. 16S sequencing to luminal and mucosal M-SHIME samples indicated that before *Lm* inoculation, the bacterial composition in all vessels was similar (Figure 3A and data not shown). In contrast, following *Lm* addition, luminal microbial community compositions were different in vessels containing WT *Lm* compared to both non-infected vessels and vessels infected with the Δ*lmo2776* isogenic mutant (Figure 3A). No difference was observed in mucosal microbial community composition. The relative abundance of 7 OTUs was lower in the case of the WT strain compared to the non-inoculated condition or upon addition of the Δ*lmo2776* strain (Figure 3B). These 7 OTUs all belonged to *Pc* species (Figure 3C), revealing that Lmo2776 targets *Pc* in human microbiota in a host-independent manner.

As short-chain fatty acid (SCFA) levels serve as a classical readout for gut microbiota metabolism and as *Prevotellae* are known to produce propionate (Flint and Duncan, 2014), we quantified SCFAs production in the luminal M-SHIME samples. A specific decrease in propionate production upon infection with WT *Lm* was observed as early as 6 h pi (Figure 3D) compared to non-infected and Δ*lmo2776*-infected vessels. This difference was continuously observed up to 3 days pi, while no significant difference was observed for butyrate, isobutyrate,

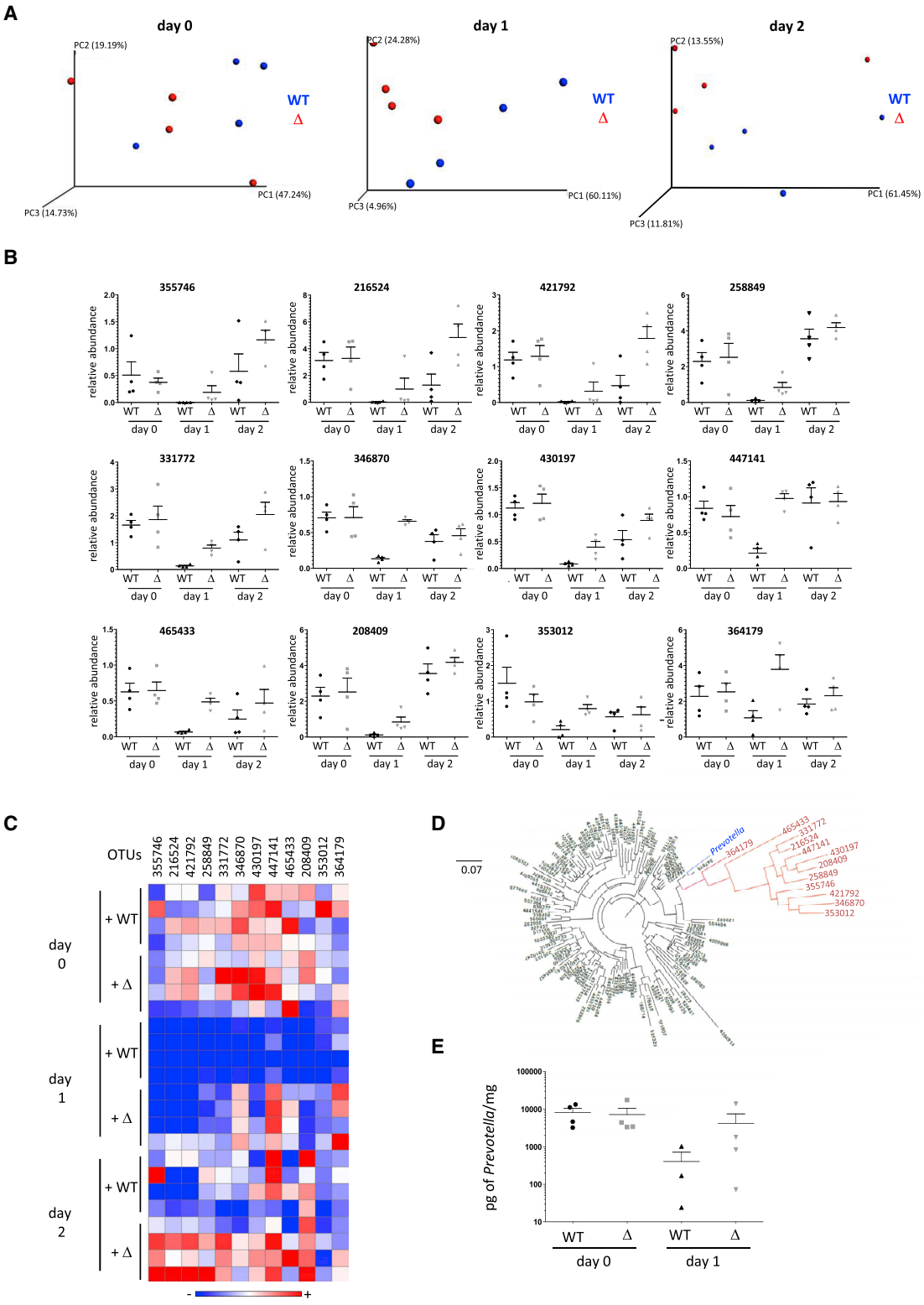

Figure 2. Lmo2776 Targets *Prevotella* in Mouse Microbiota

(A) Principal coordinates analysis of the weighted Unifrac distance matrix of mice infected with WT strain or Δ*lmo2776* at days 0, 1, and 2. Permanova: day 0, p = 0.383; day 1, p = 0.05864; and day 2, p = 0.360.

(B) Relative abundance of 12 OTUs in gut microbiota of mice inoculated with WT or Δ*lmo2776* strains overtime. Each dot represents the value for one mouse.

(legend continued on next page)

acetate and isovalerate (Figure S3). Although propionate is produced by many bacterial species, the decrease in propionate production observed upon inoculation of M-SHIME with WT *Lm* is in agreement with the decrease in *Pc* population.

Lmo2776 Targets *Pc In Vitro*

We first addressed the direct inhibitory activity of Lmo2776 on *Pc* by growing *Pc* (DSMZ 18205 strain) at 37°C in anaerobic conditions in the presence of culture supernatants of *Lm* strains and counting the viable CFUs on agar plates. Growth of *Pc* dramatically decreased in the presence of the WT *Lm* supernatant compared to the Δ*lmo2776* supernatant or medium alone (Figure 3E), suggesting that Lmo2776 is secreted and targets directly *Pc*.

To definitively assess the function of Lmo2776, a peptide of 63 aa (Gly69 to Lys131) corresponding to the putative mature form of Lmo2776 was synthesized. Its activity was first analyzed on *Pc* and *B. thetaiotaomicron* (*Bt*), another prominent commensal bacterium (Figure 3F). A dose-dependent effect of Lmo2776 peptide was observed on *Pc* growth, while no effect was observed on *Bt* growth, demonstrating that Lmo2776 targets *Pc* and not *Bt*. We then tested the effect of the peptide on several other intestinal bacteria, either aerobic (*Enterococcus faecalis*, *Escherichia coli*) or anaerobic (*Akkermansia muciniphila* [*Am*]) bacteria. No effect was observed on any of these bacteria (Figure 3G). Moreover, Lmo2776 peptide did not inhibit growth of seven other *Prevotella* species (*Ps*, *P. oris*, *P. nigrescens*, *P. pallens*, *P. corporis*, *P. melaninogenica*, and *P. bivia*). We next tested the peptide activity on 7 *Pc* isolated from healthy humans and patients. Strikingly, 6 out of the 7 strains were sensitive to the bacteriocin (Figure 3G).

We also tested the effect of the Lmo2776 peptide on known targets of the bacteriocins of the Lcn972 family (*Bacillus subtilis* [*Bs*] and *L. lactis* MG1614). Growth of *Bs* decreased significantly in presence of the peptide (Figure 3G), while no effect was observed on *L. lactis* growth. Growth of *Bs* was also significantly reduced in the presence of WT *Lm* and of Lmo2776 complemented strains compared to the Δ*lmo2776* strain (Figures S3E and S3F). Addition of the culture supernatant of WT *Lm* to *Bs* significantly decreased the number of *Bs* compared to the addition of Δ*lmo2776* culture supernatant (Figure S3G) (Li et al., 2014). Together, these results indicate that Lmo2776 is a bona fide bacteriocin that targets both *Pc* and *Bs in vitro.*

To evaluate the effect of Lmo2776 peptide *in vivo*, we used an approach previously described to bypass degradation by enzymes of the upper digestive tract. Conventional BALB/c mice were inoculated intra-rectally with Lmo2776 peptide (1mg per mice, a dose probably higher than the one produced by *Lm* upon infection) or water, taken as a control. Levels of total bacteria, *Prevotella* and *Am* were determined by qPCR on feces collected between 1 and 4 h pi. While no effect was observed on the levels of total bacteria or *Am*, fecal levels of *Prevotella* decreased following administration of Lmo2776 peptide, showing that similar to bacteria, Lmo2776 alone was effective in reducing *Pc in vivo* (Figure 3H).

Colonization of Germfree Mice by *Pc* Phenocopies the Effect of the Microbiota on *Lm* Intestinal Growth in Conventional Mice

To decipher the role of *Pc* during *Lm* infection *in vivo*, germfree C57BL/6J mice were orally inoculated with either *Pc* (DSMZ 18205 strain), *Bt* or *Ps,* another *Prevotella* present in the gut, or stably colonized with a consortium of 12 bacterial species (termed Oligo-Mouse-Microbiota (Oligo-MM^{12}), representing members of the major bacterial phyla in murine gut (Brugiroux et al., 2016)). Two weeks after colonization, mice were orally inoculated with WT *Lm* or Δ*lmo2776* strains and *Lm* loads in the intestinal lumen and target organs were compared 72 h pi. Compared to WT strain, Δ*lmo2776* mutant strain displayed significantly higher loads in the intestinal lumen (Figure 4A), spleen (Figure 4B) and liver (Figure S4) in mice colonized with *Pc*, while no difference between the two strains was observed in mice precolonized with *Bt*, *Ps* or the OligoMM^{12} consortium. In addition, the number of *Pc* significantly decreased in WT inoculated *Pc*-colonized animals compared to Δ*lmo2776*-inoculated animals (Figure 4C). Altogether, these results indicate that the greater ability of the Δ*lmo2776* mutant to grow in intestine and reach deeper tissues compared to the WT strain correlates with the presence of *Prevotella* in the microbiota, as it is observed in either conventional mice or mice colonized with *Pc*. We cannot exclude that the production of the bacteriocin against *Prevotella in vivo* and at 3 days pi has a fitness cost for *Lm* strains.

Pc Modifies the Mucus Layer

The intestinal mucus layer forms a physical barrier of about 30μm that is able to keep bacteria at a distance from the epithelium (Johansson et al., 2008). A mucus-eroding microbiota promotes greater epithelial access (Desai et al., 2016). *Prevotella*, through production of sulfatases that induce mucus degradation (Wright et al., 2000), might impair the mucosal barrier function and therefore contribute to better accessibility to intestinal epithelial cells and to local inflammation. We thus compared the colonic mucus layer thickness of conventional mice infected with WT *Lm* or Δ*lmo2776* by confocal microscopy, using mucus-preserving Carnoy fixation and FISH (Johansson and Hansson, 2012). The average distance of bacteria from colonic epithelial cells was significantly smaller in mice infected with Δ*lmo2776* compared to mice infected with WT *Lm* at 24 and 48 h (Figures 4D and 4E), suggesting that *Prevotella* present in the microbiota of mice infected with Δ*lmo2776* decreases the mucus layer thickness and might consequently increase its permeability. Of note, these distances were also smaller than in uninfected mice, indicating that *Lm* infection itself affects the mucus layer thickness. To confirm the effect of *Pc* on mucus layer in the context of listerial infection, germfree C57BL/6J mice were

(C) Heat-map analysis of the relative abundance of 12 OTUs in gut microbiota of mice inoculated with WT or Δ*lmo2776* strains. Each raw represents one mouse. The red and blue shades indicate high and low abundance.
(D) Phylogenetic tree of 16S rRNA gene alignment of 5 representative bacteria for each phylum of the bacteria domain, together with OTUs showing significantly different relative abundances in gut microbiota of mice infected with WT or Δ*lmo2776* strains at day 1 (in red).
(E) PCR quantification of *Prevotella* in feces of mice inoculated with WT strain or Δ*lmo2776* at day 0 and day 1.

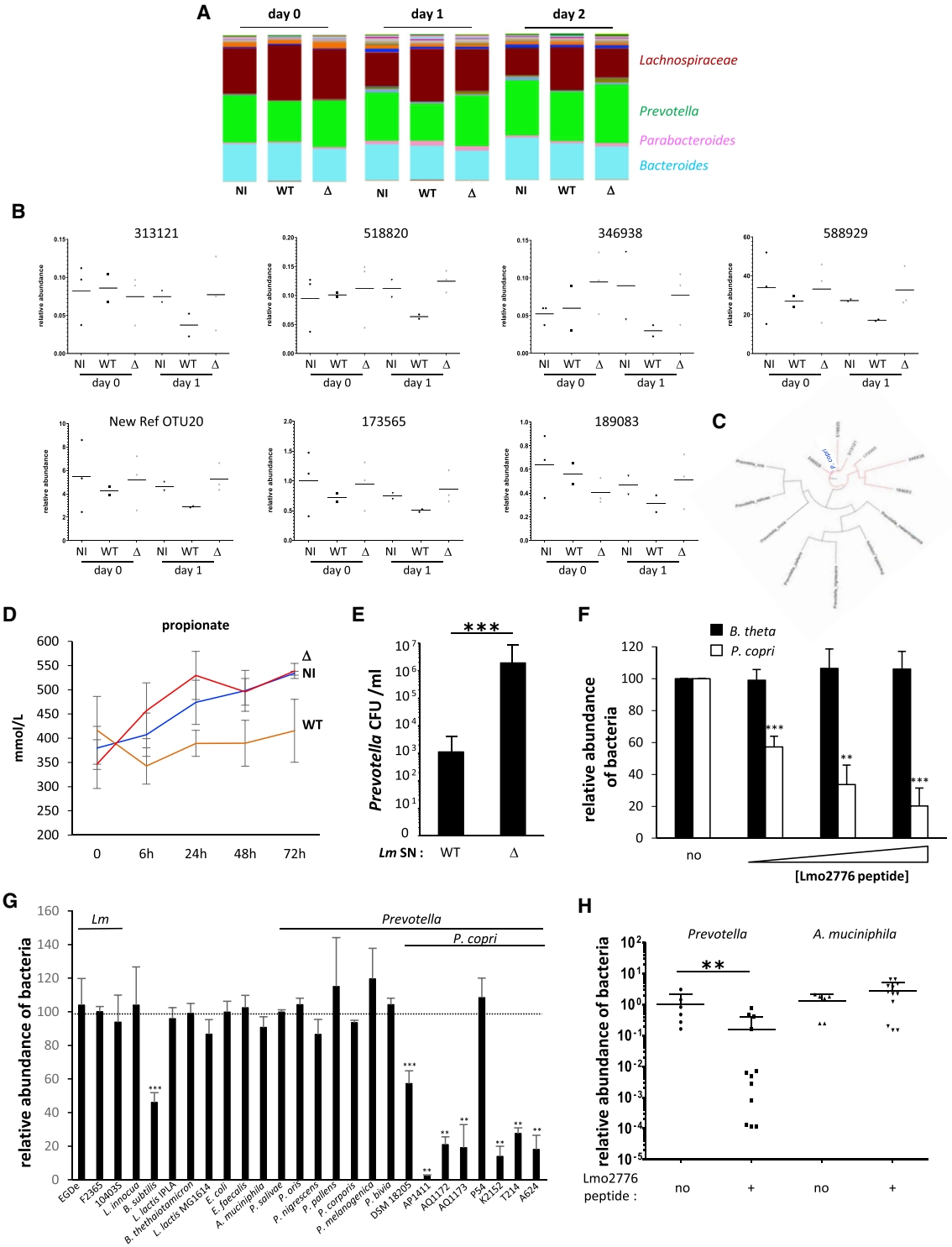

Figure 3. Lmo2776 Targets *Pc* in Human Microbiota and *In Vitro*

(A) Relative abundance of genera in SHIME vessels non-infected or infected with WT or Δ*lmo2776* strains. The four more abundant genera are indicated.

(B) Relative abundance of 7 different OTUs in SHIME vessels infected with WT or Δ*lmo2776* strains or non-infected. Each dot represents the value for one vessel.

(C) Phylogenetic tree of 16S rRNA gene alignment of several *Prevotella* species, together with OTUs showing significantly different relative abundances in vessels inoculated with WT or Δ*lmo2776* strains at day 1 (in red).

(D) Levels of propionate in SHIME vessels infected with WT or Δ*lmo2776* strains or non-infected overtime. Results are expressed as mean ± SEM for 2 to 3 individual vessels.

(legend continued on next page)

precolonized with *Pc* (DSMZ 18205 strain), *Bt*, or *Ps*, then orally inoculated with WT *Lm* or Δ*lmo2776* strains; and mucus layer thickness was analyzed by FISH. In mice precolonized with *Pc*, the average distance of bacteria from colonic epithelial cells was significantly smaller in Δ*lmo2776*-infected mice compared to WT *Lm*-infected mice (Figures 4F and 4G). Strikingly, such a difference was not observed in germfree mice or in mice precolonized with *Ps* or *Bt*, revealing that mucus erosion is dependent on *Pc*.

Since the thinner mucus layer induced by *Prevotella* could favor invasion of the host by bacteria and contribute to intestinal inflammation, we quantified faecal lipocalin-2 (LCN-2) as a marker of intestinal inflammation (Chassaing et al., 2012). LCN-2 is a small secreted innate immune protein that is critical for iron homeostasis and whose levels increase during inflammation. Faecal LCN-2 levels were analyzed after colonization of germfree mice with *Pc* compared to non-colonized mice or mice colonized with *Bt*. A significant increase of faecal LCN-2 was observed in germfree mice monocolonized with *Pc* compared to non-colonized animals or to animals monocolonized with *Bt* (Figure 4H), revealing that *Pc* induces intestinal inflammation. Altogether, these results showed that presence of *Prevotella* in the intestine is associated with a thinner mucus layer and increased levels of faecal LCN-2. They are consistent with previous reports describing *Prevotella* as a bacterium promoting a pro-inflammatory phenotype (Elinav et al., 2011; Larsen, 2017; Scher et al., 2013).

DISCUSSION

Outcompeting intestinal microbiota stands among the challenging issues for enteropathogens. Pathogens may secrete diffusible molecules such as bacteriocins or T6SS effectors to target commensals and consequently promote colonization and virulence. In most cases, molecular mechanisms underlying the interplay between pathogenic and commensal bacteria in the intestine remain elusive. We previously reported that most strains responsible for human infections, such as the F2365 strain, secrete a bacteriocin that promotes intestinal colonization by *Lm* (Quereda et al., 2016). When overexpressed in mouse gut, this bacteriocin, named Listeriolysin S (LLS), decreases *Allobaculum* and *Alloprevotella* genera known to produce butyrate or acetate, two SCFAs reported to inhibit transcription of virulence factors or growth of *Lm* (Ostling and Lindgren, 1993; Sun et al., 2012). However, whether physiological concentrations of LLS have a direct or an indirect role on these *genera* is still under investigation and is a question particularly difficult to address as LLS is highly post-translationally modified and therefore difficult to purify or to synthetize. In the case of *Salmonella enterica* serovar Typhimurium infection, killing of intestinal *Klebsiella oxytoca via* its T6SS is essential for *S. enterica* gut colonization of gnotobiotic mice colonized by *K. oxytoca* (Sana et al., 2016), but whether *K. oxytoca* and other members of the gut microbiota are targeted by the *Salmonella* T6SS in conventional mice is unknown. *Shigella sonnei* uses a T6SS to outcompete *E. coli in vivo* but the effectors responsible for this effect are unknown (Anderson et al., 2017).

Here, we report and provide evidence that the Lmo2776 *Lm* bacteriocin targets *Prevotella* in mouse and in *in vitro* reconstituted human microbiota. This effect is direct and specific to *Pc*, as (*i*) *Pc* are killed by *Lm* culture supernatant and by the purified Lmo2776 *in vitro* and (*ii*) despite the complexity of the microbiota and its well-controlled equilibrium, no other genus of the intestinal microbiota was found to be impacted by Lmo2776. By studying Lmo2776, we have unveiled a so-far-unknown role for intestinal *Pc* in exacerbating bacterial infection. The intestinal microbiota, in some cases, has already been reported to promote bacterial virulence by producing metabolites that enhance pathogens virulence gene expression and colonization in the gut (Bäumler and Sperandio, 2016; Rolhion and Chassaing, 2016). For example, *Bt* enhances *Clostridium rodentium* colonization by producing succinate (Curtis et al., 2014; Ferreyra et al., 2014), and *Am* exacerbates *S. Typhimurium*-induced intestinal inflammation by disturbing host mucus homeostasis (Ganesh et al., 2013). *Pc* decreases the mucus layer thickness and increases propionate concentration and levels of fecal LCN-2, in agreement with previous studies reporting that *Pc* exacerbates inflammation (Elinav et al., 2011; Scher et al., 2013). In addition, *Prevotella* enrichment within the lung microbiome of HIV-infected patients has been observed and is associated with Th17 inflammation (Shenoy and Lynch, 2018). *Prevotella* sp. have also been associated with bacterial vaginosis, and their role in its pathogenesis has been linked to the production of sialidase, an enzyme involved in mucin degradation and increased levels of pro-inflammatory cytokines (Briselden et al., 1992; Si et al., 2017). Together, our data strongly suggest that *Pc*, by modifying mucus layer permeability and changing the gut inflammatory condition, promotes greater epithelial access and therefore infection by *Lm* (Figure 4I). We can speculate that individuals with a high abundance of intestinal *Prevotella* might be more susceptible to enteric infections. Interestingly, it was recently shown that subjects with higher relative abundance of *Pc* could be at higher risk to traveler's diarrhea and to the carriage of multidrug-resistant *Enterobacteriaceae* (Leo et al., 2019). In addition, as Lmo2776 bacteriocin allows a selective depletion of *Pc* in the gut, it could prevent excessive inflammation and allow *Lm* persistence and long-lasting infection, eventually leading to meningitis. Further work is required to determine why *Lm*

(E) Numbers of *Pc* after incubation with supernatant of WT or Δ*lmo2776* strains.

(F) Relative abundance of *Pc* and *Bt* after 24 h incubation with increasing dose of Lmo2776 peptide (3 (+), 6 (++) and 9(+++) μg/mL) relative to their abundance without Lmo2776 peptide.

(G) Relative abundance of different bacteria after 24 h incubation with Lmo2776 peptide (3μg/mL) relative to their abundance without Lmo2776 peptide. Results are expressed as mean ± SEM of a least 3 independent experiments and P values were obtained using two-tailed unpaired Student's t test (*$p < 0.05$, ***$p < 0.005$).

(H) PCR quantification of *Prevotella* and *Am* in the feces of mice treated with Lmo2776 peptide (1 mg) or with water relative to their levels before treatment. Each dot represents the value for one mouse. Statistically significant differences were evaluated by Student's t test (**$p < 0.01$).

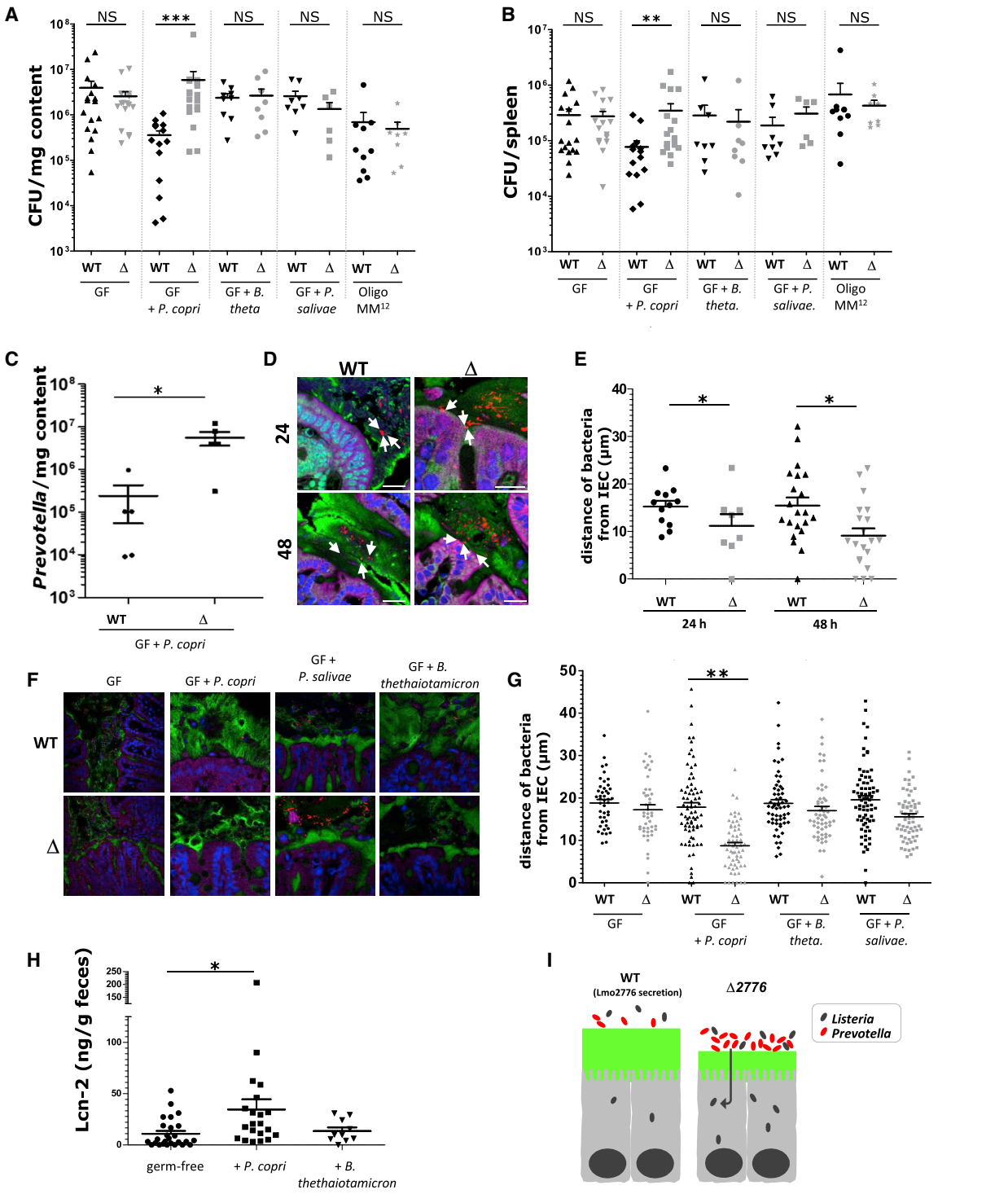

Figure 4. *Pc* Controls *Lm* Infection by Modifying Mucus Layer and Promoting Inflammation

(A and B) Assessment of listerial CFUs in the intestinal luminal content (A) and in the spleen (B) of germfree (GF) C57BL/6J mice colonized or not with *Pc, Ps* or *Bt* or stably colonized with 12 bacterial species (Oligo-MM[12]) for 2 weeks and then inoculated with *Lm* WT or Δ*lmo2776* for 72 h.

(C) Numbers of *Pc* CFUs in the intestinal luminal content of GF C57BL/6J mice colonized with *Pc* and then inoculated with *Lm* WT or Δ*lmo2776* for 72 h.

(D) Confocal microscopy analysis of microbiota localization in colon of BALB/c mice infected with *Lm* WT or Δ*lmo2776* bacteria for 24 or 48 h. Muc2 (green), actin (purple), bacteria (red), and DNA (blue). Bar = 20 μm. White arrows highlight the 3 closest bacteria. Pictures are representatives of 5 biological replicates.

(E) Distances of closest bacteria to colonic intestinal epithelial cells per condition over 5 high-powered fields per mouse, with each dot representing a measurement.

(legend continued on next page)

strains have kept the *lmo2776* gene. We showed here that the Lmo2776 bacteriocin also targets *Bs*, a Gram-positive bacterium found in the soil, suggesting that Lmo2776 could give an advantage to *Lm* in that environment. It is possible that Lmo2776 is critical for species survival and replication in a so far unknown niche, consequently favoring transmission or dissemination. *Bs* is also found in the human gastrointestinal tract (Hong et al., 2009) and could be targeted by Lmo2776 in the intestine as well. *Bs* is also targeted by Sil, another member of the Lcn972 family (Li et al., 2014). The role of the homologs of Lcn972 in other human pathogenic bacteria such as *S. pneumoniae* and *S. aureus* remains to be determined, but conservation of the bacteriocin in different pathogenic bacteria associated with mucosa strongly suggests an important role.

Taken together, our data reveal that *Pc* can modulate intestinal infection, and using Lmo2776 might represent an effective therapeutic tool for *Prevotella*-related diseases to reduce *Pc* abundance in the gut without affecting the remaining commensal microbiota.

STAR★METHODS

Detailed methods are provided in the online version of this paper and include the following:

- KEY RESOURCES TABLE
- LEAD CONTACT AND MATERIALS AVAILABILITY
- EXPERIMENTAL MODEL AND SUBJECT DETAILS
  - Bacterial Strains and Plasmids
  - Mice
- METHOD DETAILS
  - Mice Infection
  - Fecal Microbiota Analysis by 16S rRNA Gene Sequencing Using Illumina Technology
  - Bacterial Quantification in Feces
  - M-SHIME
  - RNA Extraction and qRT-PCR
  - Co-cultures and Culture in Presence of Supernatant or Lmo2776 Peptide
  - Immunostaining of Mucins and Localization of Bacteria by FISH
  - Quantification of Fecal Lcn-2 by ELISA
  - Core genome MLST
- QUANTIFICATION AND STATISTICAL ANALYSIS
  - Statistical Analysis
- DATA AND CODE AVAILABILITY
  - 16S rRNA Gene Sequence Analysis

SUPPLEMENTAL INFORMATION

Supplemental Information can be found online at https://doi.org/10.1016/j.chom.2019.10.016.

ACKNOWLEDGMENTS

We thank the CDTA (Orléans) and the Institut Pasteur Animalerie Centrale staff, especially K. Sébastien, T. Angélique, M.G. Lopez Dieguez, M. Jacob, and E. Maranghi. We thank G. Jouvion and M. Tichit for technical help and the Centre Ressources Biologiques de l'Institut Pasteur for providing strains. We thank L. Maranghi, J. Blondou, and A. Lavelle for technical support and C. Bécavin, A. Hryckowian, B. Martinez, G. Eberl, G. Hansson, and H. Sokol for helpful discussion. N.R. was supported by an EMBO short-term fellowship (ASTF 399-2015); B.C. by a Career Development Award from the CCFA, an Innovator Award from the Kenneth Rainin Foundation, and a Seed Grant from the GSU's Brain & Behavior program; H.F.-P. by an NYU-HCC CTSI grant (1TL1TR001447); and D.R.L. by the Howard Hughes Medical Institute and the Colton Center for Autoimmunity. This work was supported by grants to P.C.: ERC Advanced Grant BacCellEpi (670823), ANR (Investissement d'Avenir Programme 10-LABX-62-IBEID), ERANET Infect-ERA PROANTILIS (13-IFEC-0004-02), and the Fondation le Roch.

AUTHORS CONTRIBUTIONS

Conceptualization, P.C. and N.R.; Investigation, N.R., B.C. (16S samples preparation and sequencing data analysis, and FISH), M.-A.N. (*in vivo* work), J.d.B. (M-SHIME), A.M., and M.L. (genomic analyses); Methodology, N.R., O.D., and M.B.; Writing – Original Draft, N.R. and P.C.; Writing – Review & Editing, B.C., O.D., A.M., M.L., H.F.-P., D.R.L., M.M., A.T.G., and T.V.d.W.; Advices: O.D., A.T.G., T.V.W., and M.M.; Resources, M.B., H.F.-P., and D.R.L.; Supervision, P.C.

DECLARATION OF INTERESTS

The authors declare no competing interests.

Received: June 30, 2019
Revised: September 5, 2019
Accepted: October 23, 2019
Published: November 13, 2019

REFERENCES

Alpizar-Rodriguez, D., Lesker, T.R., Gronow, A., Gilbert, B., Raemy, E., Lamacchia, C., Gabay, C., Finckh, A., and Strowig, T. (2019). *Prevotella copri* in individuals at risk for rheumatoid arthritis. Ann. Rheum. Dis. *78*, 590–593.

An, D., Oh, S.F., Olszak, T., Neves, J.F., Avci, F.Y., Erturk-Hasdemir, D., Lu, X., Zeissig, S., Blumberg, R.S., and Kasper, D.L. (2014). Sphingolipids from a symbiotic microbe regulate homeostasis of host intestinal natural killer T cells. Cell *156*, 123–133.

Anderson, M.C., Vonaesch, P., Saffarian, A., Marteyn, B.S., and Sansonetti, P.J. (2017). Shigella sonnei Encodes a Functional T6SS Used for Interbacterial Competition and Niche Occupancy. Cell Host Microbe *21*, 769–776.

Archambaud, C., Nahori, M.A., Soubigou, G., Bécavin, C., Laval, L., Lechat, P., Smokvina, T., Langella, P., Lecuit, M., and Cossart, P. (2012). Impact of lactobacilli on orally acquired listeriosis. Proc. Natl. Acad. Sci. USA *109*, 16684–16689.

Archambaud, C., Sismeiro, O., Toedling, J., Soubigou, G., Bécavin, C., Lechat, P., Lebreton, A., Ciaudo, C., and Cossart, P. (2013). The intestinal microbiota interferes with the microRNA response upon oral Listeria infection. MBio *4*, e00707–e00713.

(F) Confocal microscopy analysis of microbiota localization in colon of GF C57BL/6J mice colonized with *Pc*, *Bt* or *Ps* for 2 weeks and inoculated with *Lm* WT or Δ*lmo2776* bacteria. Muc2 (green), actin (purple), bacteria (red), and DNA (blue). Bar: 20 μm.
(G) Distances of closest bacteria to intestinal cells per condition over 5 high-powered fields per mouse, with each dot representing a measurement.
(H) Levels of the inflammatory marker Lcn-2 in feces of mice 2 weeks pi with *Pc* or *Bt*.
(I) Model depicting the effect of *Prevotella* on *Lm* infection. In (A), (B), and (E), each dot represents one mouse. Statistically significant differences were evaluated by the Mann–Whitney test (A, B), one way-ANOVA test (E, G) or two-tailed unpaired Student's t test (C, H) (*$p < 0.05$, ***$p < 0.005$).

Arnaud, M., Chastanet, A., and Débarbouillé, M. (2004). New vector for efficient allelic replacement in naturally nontransformable, low-GC-content, gram-positive bacteria. Appl. Environ. Microbiol. *70*, 6887–6891.

Arumugam, M., Raes, J., Pelletier, E., Le Paslier, D., Yamada, T., Mende, D.R., Fernandes, G.R., Tap, J., Bruls, T., Batto, J.M., et al.; MetaHIT Consortium (2011). Enterotypes of the human gut microbiome. Nature *473*, 174–180.

Balestrino, D., Hamon, M.A., Dortet, L., Nahori, M.A., Pizarro-Cerda, J., Alignani, D., Dussurget, O., Cossart, P., and Toledo-Arana, A. (2010). Single-cell techniques using chromosomally tagged fluorescent bacteria to study Listeria monocytogenes infection processes. Appl. Environ. Microbiol. *76*, 3625–3636.

Bäumler, A.J., and Sperandio, V. (2016). Interactions between the microbiota and pathogenic bacteria in the gut. Nature *535*, 85–93.

Becattini, S., Littmann, E.R., Carter, R.A., Kim, S.G., Morjaria, S.M., Ling, L., Gyaltshen, Y., Fontana, E., Taur, Y., Leiner, I.M., and Pamer, E.G. (2017). Commensal microbes provide first line defense against *Listeria monocytogenes* infection. J. Exp. Med. *214*, 1973–1989.

Briselden, A.M., Moncla, B.J., Stevens, C.E., and Hillier, S.L. (1992). Sialidases (neuraminidases) in bacterial vaginosis and bacterial vaginosis-associated microflora. J. Clin. Microbiol. *30*, 663–666.

Brugiroux, S., Beutler, M., Pfann, C., Garzetti, D., Ruscheweyh, H.J., Ring, D., Diehl, M., Herp, S., Lötscher, Y., Hussain, S., et al. (2016). Genome-guided design of a defined mouse microbiota that confers colonization resistance against Salmonella enterica serovar Typhimurium. Nat. Microbiol. *2*, 16215.

Buffie, C.G., and Pamer, E.G. (2013). Microbiota-mediated colonization resistance against intestinal pathogens. Nat. Rev. Immunol. *13*, 790–801.

Caporaso, J.G., Lauber, C.L., Walters, W.A., Berg-Lyons, D., Huntley, J., Fierer, N., Owens, S.M., Betley, J., Fraser, L., Bauer, M., et al. (2012). Ultra-high-throughput microbial community analysis on the Illumina HiSeq and MiSeq platforms. ISME J. *6*, 1621–1624.

Chassaing, B., Srinivasan, G., Delgado, M.A., Young, A.N., Gewirtz, A.T., and Vijay-Kumar, M. (2012). Fecal lipocalin 2, a sensitive and broadly dynamic non-invasive biomarker for intestinal inflammation. PLoS One *7*, e44328.

Chassaing, B., Koren, O., Goodrich, J.K., Poole, A.C., Srinivasan, S., Ley, R.E., and Gewirtz, A.T. (2015). Dietary emulsifiers impact the mouse gut microbiota promoting colitis and metabolic syndrome. Nature *519*, 92–96.

Chassaing, B., Van de Wiele, T., De Bodt, J., Marzorati, M., and Gewirtz, A.T. (2017). Dietary emulsifiers directly alter human microbiota composition and gene expression ex vivo potentiating intestinal inflammation. Gut *66*, 1414–1427.

Curtis, M.M., Hu, Z., Klimko, C., Narayanan, S., Deberardinis, R., and Sperandio, V. (2014). The gut commensal Bacteroides thetaiotaomicron exacerbates enteric infection through modification of the metabolic landscape. Cell Host Microbe *16*, 759–769.

De Filippis, F., Pasolli, E., Tett, A., Tarallo, S., Naccarati, A., De Angelis, M., Neviani, E., Cocolin, L., Gobbetti, M., Segata, N., and Ercolini, D. (2019). Distinct Genetic and Functional Traits of Human Intestinal Prevotella copri Strains Are Associated with Different Habitual Diets. Cell Host Microbe *25*, 444–453.e3.

De Weirdt, R., Possemiers, S., Vermeulen, G., Moerdijk-Poortvliet, T.C., Boschker, H.T., Verstraete, W., and Van de Wiele, T. (2010). Human faecal microbiota display variable patterns of glycerol metabolism. FEMS Microbiol. Ecol. *74*, 601–611.

Desai, M.S., Seekatz, A.M., Koropatkin, N.M., Kamada, N., Hickey, C.A., Wolter, M., Pudlo, N.A., Kitamoto, S., Terrapon, N., Muller, A., et al. (2016). A Dietary Fiber-Deprived Gut Microbiota Degrades the Colonic Mucus Barrier and Enhances Pathogen Susceptibility. Cell *167*, 1339–1353.

Desvaux, M., Dumas, E., Chafsey, I., Chambon, C., and Hébraud, M. (2010). Comprehensive appraisal of the extracellular proteins from a monoderm bacterium: theoretical and empirical exoproteomes of Listeria monocytogenes EGD-e by secretomics. J. Proteome Res. *9*, 5076–5092.

Dillon, S.M., Lee, E.J., Kotter, C.V., Austin, G.L., Gianella, S., Siewe, B., Smith, D.M., Landay, A.L., McManus, M.C., Robertson, C.E., et al. (2016). Gut dendritic cell activation links an altered colonic microbiome to mucosal and systemic T-cell activation in untreated HIV-1 infection. Mucosal Immunol. *9*, 24–37.

Edman, D.C., Pollock, M.B., and Hall, E.R. (1968). Listeria monocytogenes L forms. I. Induction maintenance, and biological characteristics. J. Bacteriol. *96*, 352–357.

Elinav, E., Strowig, T., Kau, A.L., Henao-Mejia, J., Thaiss, C.A., Booth, C.J., Peaper, D.R., Bertin, J., Eisenbarth, S.C., Gordon, J.I., and Flavell, R.A. (2011). NLRP6 inflammasome regulates colonic microbial ecology and risk for colitis. Cell *145*, 745–757.

Ferreyra, J.A., Wu, K.J., Hryckowian, A.J., Bouley, D.M., Weimer, B.C., and Sonnenburg, J.L. (2014). Gut microbiota-produced succinate promotes C. difficile infection after antibiotic treatment or motility disturbance. Cell Host Microbe *16*, 770–777.

Flint, H.J., and Duncan, S.H. (2014). Bacteroides and Prevotella. In Encyclopedia of Food Microbiology, C.A. Batt, ed. (Elsevier), pp. 203–208.

Gaboriau-Routhiau, V., Rakotobe, S., Lécuyer, E., Mulder, I., Lan, A., Bridonneau, C., Rochet, V., Pisi, A., De Paepe, M., Brandi, G., et al. (2009). The key role of segmented filamentous bacteria in the coordinated maturation of gut helper T cell responses. Immunity *31*, 677–689.

Ganesh, B.P., Klopfleisch, R., Loh, G., and Blaut, M. (2013). Commensal Akkermansia muciniphila exacerbates gut inflammation in Salmonella Typhimurium-infected gnotobiotic mice. PLoS One *8*, e74963.

Geirnaert, A., Wang, J., Tinck, M., Steyaert, A., Van den Abbeele, P., Eeckhaut, V., Vilchez-Vargas, R., Falony, G., Laukens, D., De Vos, M., et al. (2015). Interindividual differences in response to treatment with butyrate-producing Butyricicoccus pullicaecorum 25-3T studied in an in vitro gut model. FEMS Microbiol. Ecol. *91*, fiv054.

Gilbert, J.A., Meyer, F., Jansson, J., Gordon, J., Pace, N., Tiedje, J., Ley, R., Fierer, N., Field, D., Kyrpides, N., et al. (2010). The Earth Microbiome Project: Meeting report of the "1 EMP meeting on sample selection and acquisition" at Argonne National Laboratory October 6 2010. Stand. Genomic Sci. *3*, 249–253.

Glaser, P., Frangeul, L., Buchrieser, C., Rusniok, C., Amend, A., Baquero, F., Berche, P., Bloecker, H., Brandt, P., Chakraborty, T., et al. (2001). Comparative genomics of Listeria species. Science *294*, 849–852.

Gupta, V.K., Chaudhari, N.M., Iskepalli, S., and Dutta, C. (2015). Divergences in gene repertoire among the reference Prevotella genomes derived from distinct body sites of human. BMC Genomics *16*, 153.

Herp, S., Brugiroux, S., Garzetti, D., Ring, D., Jochum, L.M., Beutler, M., Eberl, C., Hussain, S., Walter, S., Gerlach, R.G., et al. (2019). Mucispirillum schaedleri Antagonizes Salmonella Virulence to Protect Mice against Colitis. Cell Host Microbe *25*, 681–694.

Hildebrand, F., Nguyen, T.L., Brinkman, B., Yunta, R.G., Cauwe, B., Vandenabeele, P., Liston, A., and Raes, J. (2013). Inflammation-associated enterotypes, host genotype, cage and inter-individual effects drive gut microbiota variation in common laboratory mice. Genome Biol. *14*, R4.

Hong, H.A., Khaneja, R., Tam, N.M., Cazzato, A., Tan, S., Urdaci, M., Brisson, A., Gasbarrini, A., Barnes, I., and Cutting, S.M. (2009). Bacillus subtilis isolated from the human gastrointestinal tract. Res. Microbiol. *160*, 134–143.

Ivanov, I.I., Atarashi, K., Manel, N., Brodie, E.L., Shima, T., Karaoz, U., Wei, D., Goldfarb, K.C., Santee, C.A., Lynch, S.V., et al. (2009). Induction of intestinal Th17 cells by segmented filamentous bacteria. Cell *139*, 485–498.

Johansson, M.E., and Hansson, G.C. (2012). Preservation of mucus in histological sections, immunostaining of mucins in fixed tissue, and localization of bacteria with FISH. Methods Mol. Biol. *842*, 229–235.

Johansson, M.E., Phillipson, M., Petersson, J., Velcich, A., Holm, L., and Hansson, G.C. (2008). The inner of the two Muc2 mucin-dependent mucus layers in colon is devoid of bacteria. Proc. Natl. Acad. Sci. USA *105*, 15064–15069.

Jolley, K.A., and Maiden, M.C. (2010). BIGSdb: Scalable analysis of bacterial genome variation at the population level. BMC Bioinformatics *11*, 595.

Kaur, U.S., Shet, A., Rajnala, N., Gopalan, B.P., Moar, P., D, H., Singh, B.P., Chaturvedi, R., and Tandon, R. (2018). High Abundance of genus Prevotella

in the gut of perinatally HIV-infected children is associated with IP-10 levels despite therapy. Sci. Rep. *8*, 17679.

Kim, S.G., Becattini, S., Moody, T.U., Shliaha, P.V., Littmann, E.R., Seok, R., Gjonbalaj, M., Eaton, V., Fontana, E., Amoretti, L., et al. (2019). Microbiota-derived lantibiotic restores resistance against vancomycin-resistant Enterococcus. Nature *572*, 665–669.

Larsen, J.M. (2017). The immune response to Prevotella bacteria in chronic inflammatory disease. Immunology *151*, 363–374.

Lauer, P., Chow, M.Y., Loessner, M.J., Portnoy, D.A., and Calendar, R. (2002). Construction, characterization, and use of two Listeria monocytogenes site-specific phage integration vectors. J. Bacteriol. *184*, 4177–4186.

Leo, S., Lazarevic, V., Gaïa, N., Estellat, C., Girard, M., Matheron, S., Armand-Lefèvre, L., Andremont, A., Schrenzel, J., and Ruppé, E. (2019). The intestinal microbiota predisposes to traveler's diarrhea and to the carriage of multidrug-resistant Enterobacteriaceae after traveling to tropical regions. Gut Microbes *10*, 631–641.

Ley, R.E. (2016). Gut microbiota in 2015: Prevotella in the gut: choose carefully. Nat. Rev. Gastroenterol. Hepatol. *13*, 69–70.

Li, M.F., Zhang, B.C., Li, J., and Sun, L. (2014). Sil: a Streptococcus iniae bacteriocin with dual role as an antimicrobial and an immunomodulator that inhibits innate immune response and promotes S. iniae infection. PLoS One *9*, e96222.

Linnan, M.J., Mascola, L., Lou, X.D., Goulet, V., May, S., Salminen, C., Hird, D.W., Yonekura, M.L., Hayes, P., Weaver, R., et al. (1988). Epidemic listeriosis associated with Mexican-style cheese. N. Engl. J. Med. *319*, 823–828.

Lozupone, C.A., Rhodes, M.E., Neff, C.P., Fontenot, A.P., Campbell, T.B., and Palmer, B.E. (2014). HIV-induced alteration in gut microbiota: driving factors, consequences, and effects of antiretroviral therapy. Gut Microbes *5*, 562–570.

Mackanes, G.B. (1964). The Immunological Basis of Acquired Cellular Resistance. J. Exp. Med. *120*, 105–120.

Maeda, Y., Kurakawa, T., Umemoto, E., Motooka, D., Ito, Y., Gotoh, K., Hirota, K., Matsushita, M., Furuta, Y., Narazaki, M., et al. (2016). Dysbiosis Contributes to Arthritis Development via Activation of Autoreactive T Cells in the Intestine. Arthritis Rheumatol. *68*, 2646–2661.

Martínez, B., Suárez, J.E., and Rodríguez, A. (1996). Lactococcin 972 : a homodimeric lactococcal bacteriocin whose primary target is not the plasma membrane. Microbiology *142*, 2393–2398.

Maury, M.M., Tsai, Y.H., Charlier, C., Touchon, M., Chenal-Francisque, V., Leclercq, A., Criscuolo, A., Gaultier, C., Roussel, S., Brisabois, A., et al. (2016). Uncovering Listeria monocytogenes hypervirulence by harnessing its biodiversity. Nat. Genet. *48*, 308–313.

Mazmanian, S.K., Liu, C.H., Tzianabos, A.O., and Kasper, D.L. (2005). An immunomodulatory molecule of symbiotic bacteria directs maturation of the host immune system. Cell *122*, 107–118.

Mazmanian, S.K., Round, J.L., and Kasper, D.L. (2008). A microbial symbiosis factor prevents intestinal inflammatory disease. Nature *453*, 620–625.

Mellin, J.R., Tiensuu, T., Bécavin, C., Gouin, E., Johansson, J., and Cossart, P. (2013). A riboswitch-regulated antisense RNA in Listeria monocytogenes. Proc. Natl. Acad. Sci. USA *110*, 13132–13137.

Moura, A., Criscuolo, A., Pouseele, H., Maury, M.M., Leclercq, A., Tarr, C., Björkman, J.T., Dallman, T., Reimer, A., Enouf, V., et al. (2016). Whole genome-based population biology and epidemiological surveillance of Listeria monocytogenes. Nat. Microbiol. *2*, 16185.

Nguyen, T.L., Vieira-Silva, S., Liston, A., and Raes, J. (2015). How informative is the mouse for human gut microbiota research? Dis. Model. Mech. *8*, 1–16.

Ostling, C.E., and Lindgren, S.E. (1993). Inhibition of enterobacteria and Listeria growth by lactic, acetic and formic acids. J. Appl. Bacteriol. *75*, 18–24.

Pedersen, H.K., Gudmundsdottir, V., Nielsen, H.B., Hyotylainen, T., Nielsen, T., Jensen, B.A., Forslund, K., Hildebrand, F., Prifti, E., Falony, G., et al.; MetaHIT Consortium (2016). Human gut microbes impact host serum metabolome and insulin sensitivity. Nature *535*, 376–381.

Precup, G., and Vodnar, D.C. (2019). Gut *Prevotella* as a possible biomarker of diet and its eubiotic versus dysbiotic roles: a comprehensive literature review. Br. J. Nutr. *122*, 131–140.

Quereda, J.J., Dussurget, O., Nahori, M.A., Ghozlane, A., Volant, S., Dillies, M.A., Regnault, B., Kennedy, S., Mondot, S., Villoing, B., et al. (2016). Bacteriocin from epidemic Listeria strains alters the host intestinal microbiota to favor infection. Proc. Natl. Acad. Sci. USA *113*, 5706–5711.

Quévrain, E., Maubert, M.A., Michon, C., Chain, F., Marquant, R., Tailhades, J., Miquel, S., Carlier, L., Bermúdez-Humarán, L.G., Pigneur, B., et al. (2016). Identification of an anti-inflammatory protein from Faecalibacterium prausnitzii, a commensal bacterium deficient in Crohn's disease. Gut *65*, 415–425.

Rakoff-Nahoum, S., Foster, K.R., and Comstock, L.E. (2016). The evolution of cooperation within the gut microbiota. Nature *533*, 255–259.

Rolhion, N., and Chassaing, B. (2016). When pathogenic bacteria meet the intestinal microbiota. Philos. Trans. R. Soc. Lond. B Biol. Sci. *371*, 20150504.

Round, J.L., and Mazmanian, S.K. (2010). Inducible Foxp3+ regulatory T-cell development by a commensal bacterium of the intestinal microbiota. Proc. Natl. Acad. Sci. USA *107*, 12204–12209.

Sana, T.G., Flaugnatti, N., Lugo, K.A., Lam, L.H., Jacobson, A., Baylot, V., Durand, E., Journet, L., Cascales, E., and Monack, D.M. (2016). Salmonella Typhimurium utilizes a T6SS-mediated antibacterial weapon to establish in the host gut. Proc. Natl. Acad. Sci. USA *113*, E5044–E5051.

Scher, J.U., Sczesnak, A., Longman, R.S., Segata, N., Ubeda, C., Bielski, C., Rostron, T., Cerundolo, V., Pamer, E.G., Abramson, S.B., et al. (2013). Expansion of intestinal Prevotella copri correlates with enhanced susceptibility to arthritis. eLife *2*, e01202.

Shenoy, M.K., and Lynch, S.V. (2018). Role of the lung microbiome in HIV pathogenesis. Curr. Opin. HIV AIDS *13*, 45–52.

Si, J., You, H.J., Yu, J., Sung, J., and Ko, G. (2017). Prevotella as a Hub for Vaginal Microbiota under the Influence of Host Genetics and Their Association with Obesity. Cell Host Microbe *21*, 97–105.

Sun, Y., Wilkinson, B.J., Standiford, T.J., Akinbi, H.T., and O'Riordan, M.X. (2012). Fatty acids regulate stress resistance and virulence factor production for Listeria monocytogenes. J. Bacteriol. *194*, 5274–5284.

Van den Abbeele, P., Roos, S., Eeckhaut, V., MacKenzie, D.A., Derde, M., Verstraete, W., Marzorati, M., Possemiers, S., Vanhoecke, B., Van Immerseel, F., and Van de Wiele, T. (2012). Incorporating a mucosal environment in a dynamic gut model results in a more representative colonization by lactobacilli. Microb. Biotechnol. *5*, 106–115.

Van den Abbeele, P., Belzer, C., Goossens, M., Kleerebezem, M., De Vos, W.M., Thas, O., De Weirdt, R., Kerckhof, F.M., and Van de Wiele, T. (2013). Butyrate-producing Clostridium cluster XIVa species specifically colonize mucins in an in vitro gut model. ISME J. *7*, 949–961.

Wright, D.P., Rosendale, D.I., and Robertson, A.M. (2000). Prevotella enzymes involved in mucin oligosaccharide degradation and evidence for a small operon of genes expressed during growth on mucin. FEMS Microbiol Lett. *190*, 73–79.

STAR★METHODS

KEY RESOURCES TABLE

REAGENT or RESOURCE	SOURCE	IDENTIFIER
Antibodies		
Mucin-2 primary antibody	Santa Cruz Biotechnology	rabbit H-300
Bacterial and Virus Strains		
EGD-e *Listeria monocytogenes* WT strain	Mackanes, 1964	BUG 1600
EGD-e Δ*lmo2776* *Listeria monocytogenes* EGD-e *lmo2776* deletion mutant	this study	BUG 3713
EGD-e Δ*lmo2776* p*lmo2776* pAD-lmo2776 chromosomally integrated in Δ*lmo2776*	this study	BUG 3717
F2365, *Listeria monocytogenes* strain associated with the 1985 listeriosis outbreak in California	Linnan et al., 1988	BUG 3012
10403S, *Listeria monocytogenes* WT strain	Edman et al., 1968	BUG 1361
L. innocua Clip11262	ATCC	ATCC 33091
Bacillus subtilis 168trpC2	Institut Pasteur Collection	BUG 748
Escherichia coli Top10	Invitrogen	C404003
Bacteroides thethaiotamicron	Institut Pasteur Collection	CIP 104206T
Lactococcus lactis IL14103	Gift from B. Martinez	BUG 1801
Lactococcus lactis M1363	Gift from B. Martinez	BUG 3029
Enterococcus faecalis	ATCC	ATCC 700802
Akkermensia muciniphila	ATCC	ATCC BA-835
Prevotella copri	DSMZ	DSMZ 18205
Prevotella salivae	DSMZ	DSMZ 15606
Prevotella oris	Institut Pasteur Collection	CIP 104480T
Prevotella nigrescens	Institut Pasteur Collection	CIP 105552T
Prevotella pallens	Institut Pasteur Collection	CIP 105551T
Prevotella corporis	Institut Pasteur Collection	CIP 105107T
Prevotella melanogenica	Institut Pasteur Collection	CIP 104591
Prevotella bivia	Institut Pasteur Collection	CIP 105105T
Chemicals, Peptides, and Recombinant Proteins		
GTFWVTWGQDRHYSNYQHTKKTHRSSASNYRATERSSW KAKNNLATAWIKSSLWGNKANWATK	Chemically synthetized polypeptide for this study	N/A
Critical Commercial Assays		
PowerSoilTM DNA Isolation Kit	MOBiO	12888-50
Quant-iT PicoGreen dsDNA assay	ThermoFischer	P7589
Deposited Data		
16S rRNA gene sequence data	this study	in the European Nucleotide Archive database (https://www.ebi.ac.uk/ena)
Experimental Models: Organisms/Strains		
BALB/c mice	Charles River	24980676
C57BL6/J mice	Charles River	24980803
Oligonucleotides		
All oligonucleotides are listed in Table S1.	This study	N/A
Recombinant DNA		
pMAD(shuttle vector used for creating plasmid for mutagenesis)	Arnaud et al., 2004	N/A
pAD (site-specific integration vector used for complementation)	Lauer et al., 2002	N/A
p*lmo2776 lmo2776* complementation plasmid	this study	N/A

(*Continued on next page*)

Continued

REAGENT or RESOURCE	SOURCE	IDENTIFIER
Software and Algorithms		
GraphPad Prism 6.0	GraphPad Software	https://www.graphpad.com/scientific-software/prism/
Microsoft Excel	Microsoft	https://products.office.com/en-us/excel

LEAD CONTACT AND MATERIALS AVAILABILITY

Further information and requests for resources and reagents, including strains and plasmids generated in this study, should be directed to and will be fulfilled by the Lead Contact, Pascale Cossart (pascale.cossart@pasteur.fr). All reagents generated in this study are available from the Lead Contact.

EXPERIMENTAL MODEL AND SUBJECT DETAILS

Bacterial Strains and Plasmids

Strains, plasmids and primers used in this study are listed in in the Key Resources Table. For standard experiments, *Listeria*, *E. coli*, *Bs* and *L. lactis* were grown at 37°C with shaking in Brain Heart Infusion (BHI) medium (Difco) and Luria-Bertani (LB) medium (BD). If needed, *Lm* were selected on Oxford medium (Oxoid). Anaerobic bacteria were grown in appropriate medium (PYG medium modified or Schaedler medium or BHI supplemented with 8mM L-Cysteine hydrochloride, 0.2% $NaHCO_3$ and 0.025% Hemin, following ATCC or DSMZ recommendations) at 37°C under anaerobic conditions (Genbag Anaer, Biomérieux or AnaeroGen, ThermoScientific). The Lmo2776 deletion mutant was constructed using the pMAD shuttle plasmid (Arnaud et al., 2004) as described previously (Mellin et al., 2013) and confirmed by DNA sequencing. For the construction of pAD-based plasmid, fragment obtained by PCR with EGD-e genomic DNA as template, was cloned into the SmaI/SalI sites of the pAD vector (Balestrino et al., 2010) derived previously from the pPL2 vector (Lauer et al., 2002). Plasmid was verified by sequencing with primers pPL2-Rv and pPL2-Fw and were transformed into Δ*lmo2776* by electroporation. Integration in the chromosome was verified by PCR using primers NC16 and PL95 (Balestrino et al., 2010). *Pc* strains (AP1411, AQ1172, AQ1173, P54, K2152, T214 and A624) were isolated from stool from healthy subjects and new onset rheumatoid arthritis patients. Stool was collected into anaerobic transport media (Anaerobe Systems), then streaked on BRU and LKV plates (Anaerobe Systems). After 24-48 h, individual colonies were picked and screened with *Prevotella*-specific PCR primers, and the 16S rRNA V3-V4 sequence was confirmed by Sanger sequencing (Fehlner-Peach et al., manuscript in preparation). *Prevotella*-positive isolates were grown on BRU plates, and glycerol stocks were frozen at −80°C.

Mice

9- to 12-week-old female BALB/c conventional (Charles River) or C57BL6/J conventional (Charles River) or C57BL6/J germfree (CDTA or Pasteur) or C57BL6/J stably colonized with a consortium of 12 bacterial species (termed Oligo-Mouse-Microbiota (Oligo-MM^{12}), representing members of the major bacterial phyla in the murine gut: *Bacteroidetes* (*Bacteroides caecimuris* and *Muribaculum intestinale*), *Proteobacteria* (*Turicimonas muris*), *Verrucomicrobia* (*Am*), *Actinobacteria* (*Bifidobacterium longum subsp. Animalis*) and *Firmicutes* (*Enterococcus faecalis, Lactobacillus reuteri, Blautia coccoides, Flavonifractor plautii, Clostridium clostridioforme, Acutalibacter muris* and *Clostridium innocuum*) (Brugiroux et al., 2016)) mice were used for experiments. Germfree and Oligo-MM^{12} mice were housed in plastic gnotobiotic isolators.

All animal experiments were carried out in strict accordance with the French national and European laws and conformed to the Council Directive on the approximation of laws, regulations, and administrative provisions of the Member States regarding the protection of animals used for experimental and other scientific purposes (86/609/Eec). Experiments that relied on laboratory animals were performed in strict accordance with the Institut Pasteur's regulations for animal care and use protocol, which was approved by the Animal Experiment Committee of the Institut Pasteur (approval no. 03-49).

METHOD DETAILS

Mice Infection

Lm overnight cultures were diluted in BHI and bacteria were grown to an optical density at 600 nm (OD600) of 1. Bacterial cultures were centrifuged at 3,500 × g for 15 min and washed three times in phosphate-buffered saline (PBS). Mice were infected orally with 5×10^9 bacteria diluted in 200 μl of PBS supplemented with 300 μl of $CaCO_3$ (50 mg/mL). Serial dilutions of the inoculum were plated to control the number of bacteria inoculated. The different inoculum were closed to 5×10^9 bacteria and the mean ± SEM of all independent experiments were: for WT: $5.03 \times 10^9 \pm 0.26 \times 10^9$, for Δ*lmo2776*: $5.01 \times 10^9 \pm 0.14 \times 10^9$ ($p = 0.45$) or Lmo2776 complemented strain: $4.87 \times 10^9 \pm 0.30 \times 10^9$ ($p = 0.25$). Mice were killed at subsequent time points, and intestines, spleens, and livers were removed. The small intestine was opened, and the luminal content was recovered in a 1.5-mL tube and weighed. The small intestine (duodenum, jejunum, and ileum) tissue was washed four times in DMEM (ThermoFisher), incubated for 2 h in DMEM

supplemented with 40 μg/mL gentamycin, and finally washed four times in DMEM. All of the organs and the intestinal luminal content were homogenized, serially diluted, and plated onto BHI plates or Oxford plates and grown overnight at 37°C for 48–72 h. CFU were enumerated to assess bacterial load. At least three independent experiments were carried out with four or five mice per group in each experiment. Statistically significant differences were evaluated by the Mann–Whitney test, and differences were considered statistically significant when P values were < 0.05.

For mice colonization, *Pc*, *Ps* and *Bt* were grown to log phase under anaerobic conditions in PYG modified or Schaedler broth media and 10^7 CFU were used to inoculate germ-free mice. Feces were collected at 2 weeks post-gavage to confirm colonization. Feces were homogenized, serially diluted and plated on PYG modified, Schaedler or Columbia agar plates.

Six- to 8-week-old female BALB/c mice (Charles River, Inc., France) were injected intravenously with 5.10^3 CFU of the indicated strain. Mice were sacrificed at 72 h after infection, and livers and spleens were removed. Organs were homogenized and serially diluted. Dilutions were plated onto BHI plates and grown during 24 h at 37°C. Colonies were counted to assess bacterial load per organ.

Fecal Microbiota Analysis by 16S rRNA Gene Sequencing Using Illumina Technology

Before infection, 8 BALB/c conventional mice were co-housed for 5 weeks in order to stabilize and homogenize their microbiota. After oral infection, animals were single-housed. Feces were collected and frozen at −20°C. 16S rRNA gene amplification and sequencing were done using the Illumina MiSeq technology following the protocol of Earth Microbiome Project with their modifications to the MOBIO PowerSoil DNA Isolation Kit procedure for extracting DNA (Caporaso et al., 2012; Gilbert et al., 2010). Bulk DNA were extracted from frozen extruded feces using a PowerSoil DNA Isolation kit (MoBio Laboratories) with mechanical disruption (bead-beating). The 16S rRNA genes, region V4, were PCR amplified from each sample as described in Chassaing et al., 2015 (Chassaing et al., 2015). Four independent PCRs were performed for each sample, combined, purified with Ampure magnetic purification beads (Agencourt), and products were visualized by gel electrophoresis. Products were then quantified (BIOTEK Fluorescence Spectrophotometer) using Quant-iT PicoGreen dsDNA assay. A master DNA pool was generated from the purified products in equimolar ratios. The pooled products were quantified using Quant-iT PicoGreen dsDNA assay and then sequenced using an Illumina MiSeq sequencer (paired-end reads, 2 × 250 bp) at Cornell University (Ithaca, USA).

Bacterial Quantification in Feces

Bulk DNA were extracted from frozen extruded feces using a PowerSoil DNA Isolation kit (MoBio Laboratories) with mechanical disruption (bead-beating). q-PCR reactions were prepared with SYBR Green master mix. Reaction cycling and quantification was carried out in an C1000 touch Thermal cycler (CFX384, Biorad). Genomic DNA from *Prevotella* was used to generate a standard curve to quantitate pg of *Prevotella* present per mg of total feces.

M-SHIME

M-SHIME system is a dynamic *in vitro* model which simulates the lumen-associated and mucus-associated human intestinal microbial ecosystem (ProDigest, Ghent University, Belgium) (Geirnaert et al., 2015; Van den Abbeele et al., 2013; Van den Abbeele et al., 2012). It consists of consecutive pH-controlled, stirred, airtight, double-jacketed glass vessels kept at 37°C and under anaerobic conditions. The system was operated as described earlier (Chassaing et al., 2017) with minor modifications The set-up used here consisted of 3 stomach-small intestine vessels and 9 proximal colon vessels in parallel (3 for non-infected condition, 3 for infection with WT and 3 for infection with Δ*lmo2776*). The colon vessels were inoculated at the start with 40 mL fresh human faecal suspension, from a healthy volunteer with high levels of *Prevotella*, in 500 mL sterile nutritional medium. Every 2 days, half of the mucin agar-covered microcosms were replaced by fresh sterile ones under a flow of N_2 to prevent disruption of anaerobic conditions. Fourteen days after inoculation, 3 colon vessels were infected with 10^6 WT bacteria, 3 colon vessels with 10^6 Δ*lmo2776* and 3 were left uninfected. Lumen (10 ml) and mucin agar samples were taken at 6, 24, 48 and 72 h. Mucin agar-covered microcosms were washed with sterile PBS to remove lumen bacteria. Mucin agar was removed from microcosms, homogenized and stored immediately at −20°C until further analysis.

For 16S rRNA Gene Sequencing, DNA was extracted from 1 mL of lumen samples or 250 mg of mucin agar samples using a PowerSoil DNA Isolation kit and 16S rRNA gene sequencing was analyzed as decribed above.

Our full 16S rRNA gene sequence data are deposited under Study ID PRJEB34638 in the European Nucleotide Archive database (https://www.ebi.ac.uk/ena).

For SCFA analysis, lumen samples were diluted 1:2 in demineralized water. Acetate, propionate, butyrate, isobutyrate and isovalerate were extracted and quantified as described (De Weirdt et al., 2010).

RNA Extraction and qRT-PCR

A total of 25 mL cultures of bacteria, grown in BHI, was pelleted for 20 min at 3000 g. Pellets were resuspended in 1 mL TRI Reagent (Sigma), transferred to 2 mL Lysing Matrix tubes (MP Biomedicals) and mechanically lysed by bead beating in a FastPrep apparatus (twice 45 s, speed 6.5). Tubes were then centrifuged for 5 min at 8000 g at 4°C to separate beads from lysates. The lysates were drawn off and transferred to a 2 mL Eppendorf tube. 200 uL chloroform was added to the lysate, shaken and incubated 10 min at room temperature, followed by centrifugation for 15 min at 13 000 g at 4°C. The aqueous phase was transferred to a new tube and RNA was precipitated by the addition of 500 uL isopropanol and incubation at room temperature for 10 min. RNA was pelleted

by centrifuging for 10 min at 13000 g at 4°C, washed twice with 75% ethanol. RNA pellets were resuspended in 50 to 100 uL water. For each sample, 10 ug of RNA was treated with Dnase (Turbo DNA-free, Ambion) following manufacturer's instructions. cDNA was synthetiszed from 1 ug of RNA using QuantiTect Reverse Transcription (QIAGEN) and reactions were subsenquently diluted with 180 ul of water. qRT-PCR reactions were prepared with SYBR Green master mix. Reaction cycling and quantification was carried out in an C1000 touch Thermal cycler (CFX384, Biorad). Expression levels were normalized to the *rpoB* gene. Samples were evaluated in triplicate and results represent at least three independent experiments.

Co-cultures and Culture in Presence of Supernatant or Lmo2776 Peptide

For co-culture assays with *Bs*, a mixture of equivalent CFU (10^7) of *Bs* and *Lm* (WT, Δ*lmo2776* or p2776) was inoculated into 5 mL of fresh BHI and incubated at 37°C for 6 h. Serial dilutions were plated on BHI and on Oxford media for CFU enumeration.

For culture of target in presence of *Listeria* supernatant, 25 mL of overnight culture of *Listeria* were centrifuged at 13000 g and the supernatants were collected and centrifuged further to remove cells and cells debris. Supernatants were filtered through a 0.20μm pore size filter (Millipore). 10^7 bacterial targets (*Bs*, *E. coli* or *Pc*) were inoculated at 37°C into 2.5 mL of listerial supernatant and 2.5 mL of fresh medium (BHI for *Bs*, LB for *E. coli* and PYG modified for *Pc*). At 16 h after inoculation (in aerobic conditions for *Bs* and *E. coli* and in anaerobic conditions for *Pc*), cultures were serially diluted and plated on medium.

For *in vitro* assays, a peptide of 63aa (GTFWVTWGQDRHYSNYQHTKKTHRSSASNYRATERSSWKAKNNLATAWIKSSLWGN KANWATK), corresponding to the putative mature form of Lmo2776 has been chemically synthesized (Polypeptide) and diluted. 10^7 bacteria were inoculated in absence or in presence of different concentrations of this peptide at 37°C into 5 mL of medium. At 16 h after inoculation (in aerobic or anaerobic conditions), cultures were serially diluted and plated.

For *in vivo* assays, conventional mice were anaesthetized with an intraperitoneal injection of 75 mg ketamine kg^{-1} and 5 mg xylazine kg^{-1}. One hundred ul of Lmo2776 peptide (1mg in 100μl distilled H_2O) was introduced rectally using a flexible catheter into each of 12 test mice and 100μl distilled H_2O was introduced into each of 6 control mice. Feces were collected between 1 and 4 h following the introduction. Bacteria were quantified as described above.

Immunostaining of Mucins and Localization of Bacteria by FISH

Colonic mucus immunostaining was paired with fluorescent *in situ* hybridization (FISH), as previously described (Chassaing et al., 2017; Johansson and Hansson, 2012). Briefly, colonic tissues (proximal colon, 2nd cm from the cecum) containing fecal material were placed in methanol-Carnoy's fixative solution (60% methanol, 30% chloroform, 10% glacial acetic acid) for a minimum of 3 h at room temperature. Tissues were then washed in methanol 2 × 30 min, ethanol 2 × 15 min, ethanol/xylene (1:1) 15 min and xylene 2 × 15 min, followed by embedding in Paraffin with a vertical orientation. Five μm sections were performed and dewax by preheating at 60°C for 10 min, followed by xylene 60°C for 10 min, xylene for 10 min and 99.5% ethanol for 10 min. Hybridization step was performed at 50°C overnight with EUB338 probe (5′-GCTGCCTCCCGTAGGAGT-3′, with a 5′ labeling using Alexa 647) diluted to a final concentration of 10 μg/mL in hybridization buffer (20 mM Tris–HCl, pH 7.4, 0.9 M NaCl, 0.1% SDS, 20% formamide). After washing 10 min in wash buffer (20 mM Tris–HCl, pH 7.4, 0.9 M NaCl) and 3 × 10 min in PBS, PAP pen (Sigma-Aldrich) was used to mark around the section and block solution (5% fetal bovine serum in PBS) was added for 30 min at 4°C. Mucin-2 primary antibody (rabbit H-300, Santa Cruz Biotechnology, Dallas, TX, USA) was diluted 1:1500 in block solution and apply overnight at 4°C. After washing 3 × 10 min in PBS, block solution containing anti-rabbit Alexa 488 secondary antibody diluted 1:1500, Phalloidin-Tetramethylrhodamine B isothiocyanate (Sigma-Aldrich) at 1 μg/mL and Hoechst 33258 (Sigma-Aldrich) at 10 μg/mL was applied to the section for 2 h. After washing 3 × 10 min in PBS slides were mounted using Prolong anti-fade mounting media (Life Technologies, Carlsbad, CA, USA). Observations were performed with a Zeiss LSM 700 confocal microscope. The software Zen 2011 version 7.1 was used to measure the distance between bacteria and epithelial cell monolayer.

Quantification of Fecal Lcn-2 by ELISA

Fecal samples were weighted, reconstituted in PBS-0.1% Tween 20 to a final concentration of 100 mg/mL and homogenized. Samples were then centrifuged for 10 min at 14 000 g and 4°C and supernatants were collected and stored at −20°C until analysis. Lcn-2 levels were measured using DuoSet mouse Lipocalin-2/NGAL ELISA kit (R&D Systems).

Core genome MLST

lmo2774, *lmo2775*, *lmo2776* genes were screened in a collection of 1,696 publicly available genomes (Moura et al., 2016)representative of the diversity of lineages and sublineages of *Lm*. Genes were detected using the BLASTn algorithm implemented in BIGSdb-Lm platform v.1.17 (https://bigsdb.pasteur.fr/listeria; (Jolley and Maiden, 2010; Moura et al., 2016), with minimum nucleotide identity of 70%, alignment length coverage of 70% and word size of 10.

QUANTIFICATION AND STATISTICAL ANALYSIS

Statistical Analysis

Statistically significant differences were evaluated by Mann–Whitney test, one way-ANOVA test or two-tailed unpaired Student's t test using Excel or Prism software. Statistical details of experiments and statistical tests are reported and described in the figure legends. Differences denoted in the text as significant fall below a p value of 0.05.

DATA AND CODE AVAILABILITY

16S rRNA Gene Sequence Analysis

Analysis of the 16S rRNA gene sequence was performed exactly as previously described (Chassaing et al., 2015). Our full 16S rRNA gene sequence data are deposited under Study ID PRJEB34638 in the European Nucleotide Archive database (https://www.ebi.ac.uk/ena).

Cell Host & Microbe, Volume *26*

Supplemental Information

A *Listeria monocytogenes* Bacteriocin Can Target the Commensal *Prevotella copri* and Modulate Intestinal Infection

Nathalie Rolhion, Benoit Chassaing, Marie-Anne Nahori, Jana de Bodt, Alexandra Moura, Marc Lecuit, Olivier Dussurget, Marion Bérard, Massimo Marzorati, Hannah Fehlner-Peach, Dan R. Littman, Andrew T. Gewirtz, Tom Van de Wiele, and Pascale Cossart

Supplemental information

Figure S1. Related to Figure 1. (**A**) Schematic representation of the *lmo2776* genetic region. **(B)** Amino acid alignment of Lmo2776 with members of the Lnc972 family: L82330 from *Lactococcus lactis* subsp. *lactis* Il1403, SP_0109 bacteriocin from *Streptococcus pneumoniae* TIGR4, SAP109 from *Staphylococcus aureus* subsp. *aureus* N315, lcn972 lactococcin 972 from *Lactococcus lactis* subsp. *lactis* and Sil from *Streptococcus iniae* SF. The conserved residues and consensus motif are indicated in color and on the bottom, respectively. **(C)** Cluster analysis based on core genome multilocus sequence typing (cgMLST) profiles of 1,696 genomes (obtained from Moura et al., 2016) and distribution of lmo2774-lmo2775-lmo2776 genes (in blue) across *Lm* phylogenetic lineages. The ten most frequent sublineages (SL) are highlighted. The serogroup and sample source are shown in the first and last columns, respectively, using the color code indicated in the upper right key. **(D)** Relative expression of *lmo2774*, *lmo2775* and *lmo2776* in bacteria grown in stationary phase (white bars) compared to bacteria grown in exponential phase (black bars). The transcripts levels were normalised to the levels of *rpoB*, which were constant under all conditions, and then expressed relative to those of exponential phase. Results are expressed as mean ± SEM of a least 3 independent experiments and P-values were obtained using two-tailed unpaired Student's t-test (*$p<0.05$). **(E)** Relative expression of *lmo2774*, *lmo2775* and *lmo2777* in Δ*lmo2776* bacteria compared to WT bacteria, grown in exponential phase (black bars) or in stationary phase (grey bars). The transcripts levels were normalised to the levels of *rpoB*, which were constant under all conditions. Results are expressed as mean ± SEM of a least 3 independent experiments. **(F)** Growth curves of WT and Δ*lmo2776* bacteria at 37°C with shaking in BHI. **(G)** BALB/c mice were inoculated orally with *Lm* WT (EGDe) or Δ*lmo2776* bacteria. CFUs in the intestinal luminal content were assessed at 24, 48 and 72h pi. **(H)** BALB/c mice were inoculated intravenously with WT or Δ*lmo2776* bacteria. CFUs in the spleen and the liver were assessed at 72h pi. Each dot represents the value for one mouse. Statistically significant differences were evaluated by the Mann–Whitney test. (*$p< 0.05$).

Figure S2. Related to Figure 2. (**A**) Principal coordinates analysis of the weighted Unifrac distance matrix of conventional mice at day 0 (red) and infected with WT strain at day 1 (blue). Permanova P= 0.002. (**B**) Relative abundance of classes in conventional mice at day 0 (left) and infected with WT strain at day 1 (right). LEfSE (**C**) and histogram of the LDA scores (**D**) computed for features differentially abundant between microbiota of mice at day 0 (red) and

infected with WT strain at day 1 (green). (**E**) Firmicutes/Bacteroides ratio in microbiota of mice at day 0 and infected with WT strain at day 1. Each dot represents the value for one mouse.

Figure S3. Related to Figure 3. Levels of butyrate (**A**), isobutyrate (**B**), acetate (**C**) and isovalerate (**D**) in SHIME® vessels infected with WT or Δ*lmo2776* strains or non-infected overtime. Results are expressed as mean ± SEM for 2 to 3 individual vessels. Numbers of *Bs* (**E**) and of different *Lm* strains (**F**) were quantified after 6h of co-culture. Numbers of *Bs* or *E. coli* (**G**) after incubation with supernatant of WT or Δ*lmo2776* strains. Results are expressed as mean ± SEM of a least 3 independent experiments and P-values were obtained using two-tailed unpaired Student's t-test (*$p<0.05$, ***$p<0.005$).

Figure S4. Related to Figure 4. Assessment of listerial CFUs in the liver of germfree (GF) C57BL/6J mice colonized or not with *Pc*, *Ps* or *Bt* or stably colonized with 12 bacterial species (Oligo-MM^{12}) for 2 weeks and then inoculated with *Lm* WT or Δ*lmo2776* for 72h. Each dot represents one mouse.

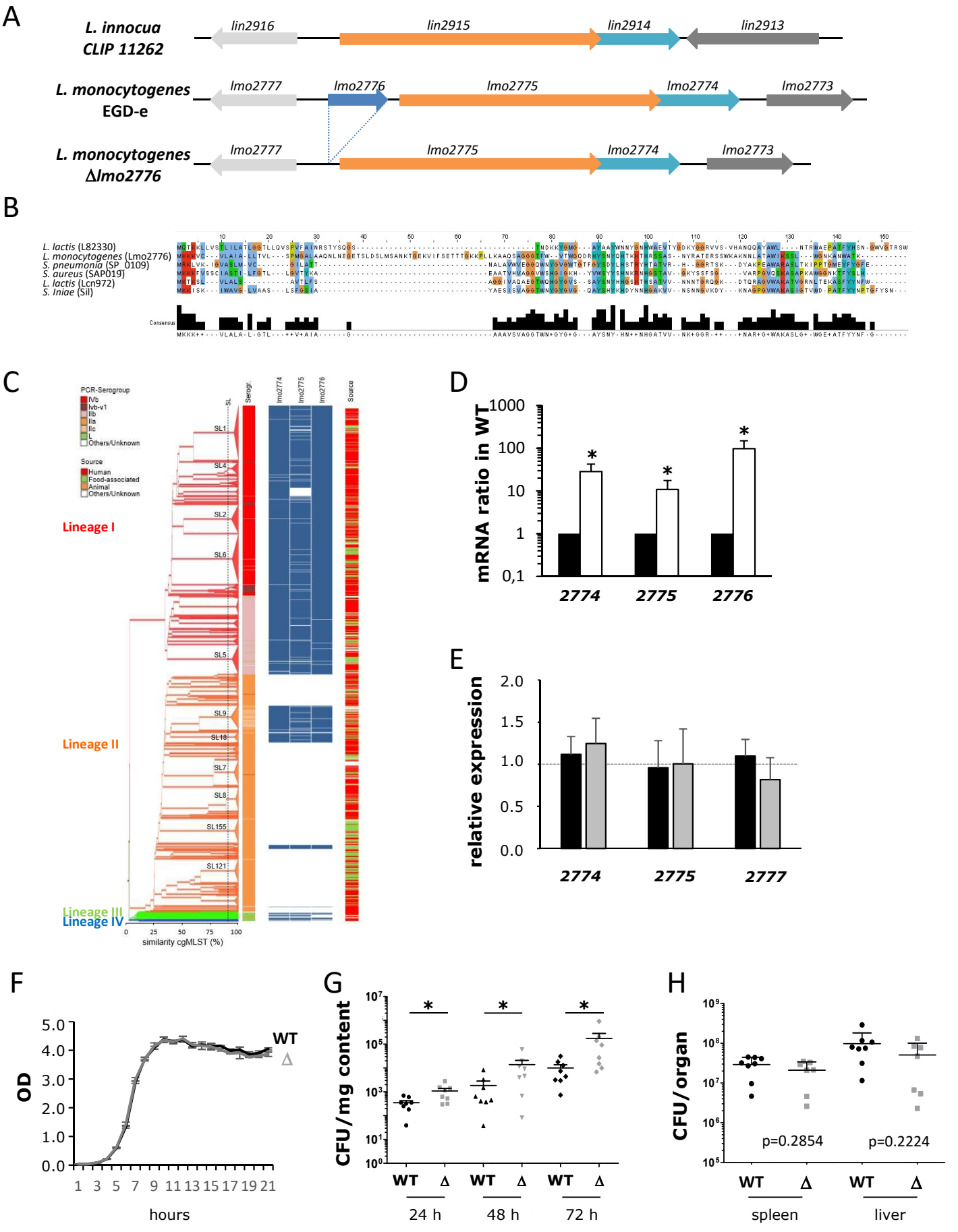
A
L. innocua CLIP 11262
lin2916
lin2915
lin2914
lin2913
L. monocytogenes EGD-e
lmo2777
lmo2776
lmo2775
lmo2774
lmo2773
L. monocytogenes ΔImo2776
lmo2777
lmo2775
lmo2774
lmo2773
B
L. lactis (L82330)
L. monocytogenes (Lmo2776)
S. pneumonia (SP_0109)
S. aureus (SAP019)
L. lactis (Lcn972)
S. Iniae (Sil)
Consensus
C
PCR-Serogroup
IVb
IVb-v1
IIb
IIa
IIc
L
Others/Unknown
Source
Human
Food-associated
Animal
Others/Unknown
Serogr.
lmo2774
lmo2775
lmo2776
Source
Lineage I
Lineage II
Lineage III
Lineage IV
SL1
SL4
SL2
SL6
SL5
SL9
SL18
SL7
SL8
SL155
SL121
similarity cgMLST (%)
D
mRNA ratio in WT
2774
2775
2776
E
relative expression
2774
2775
2777
F
OD
WT
Δ
hours
G
CFU/mg content
WT
Δ
24 h
48 h
72 h
H
CFU/organ
p=0.2854
p=0.2224
spleen
liver

Figure S1

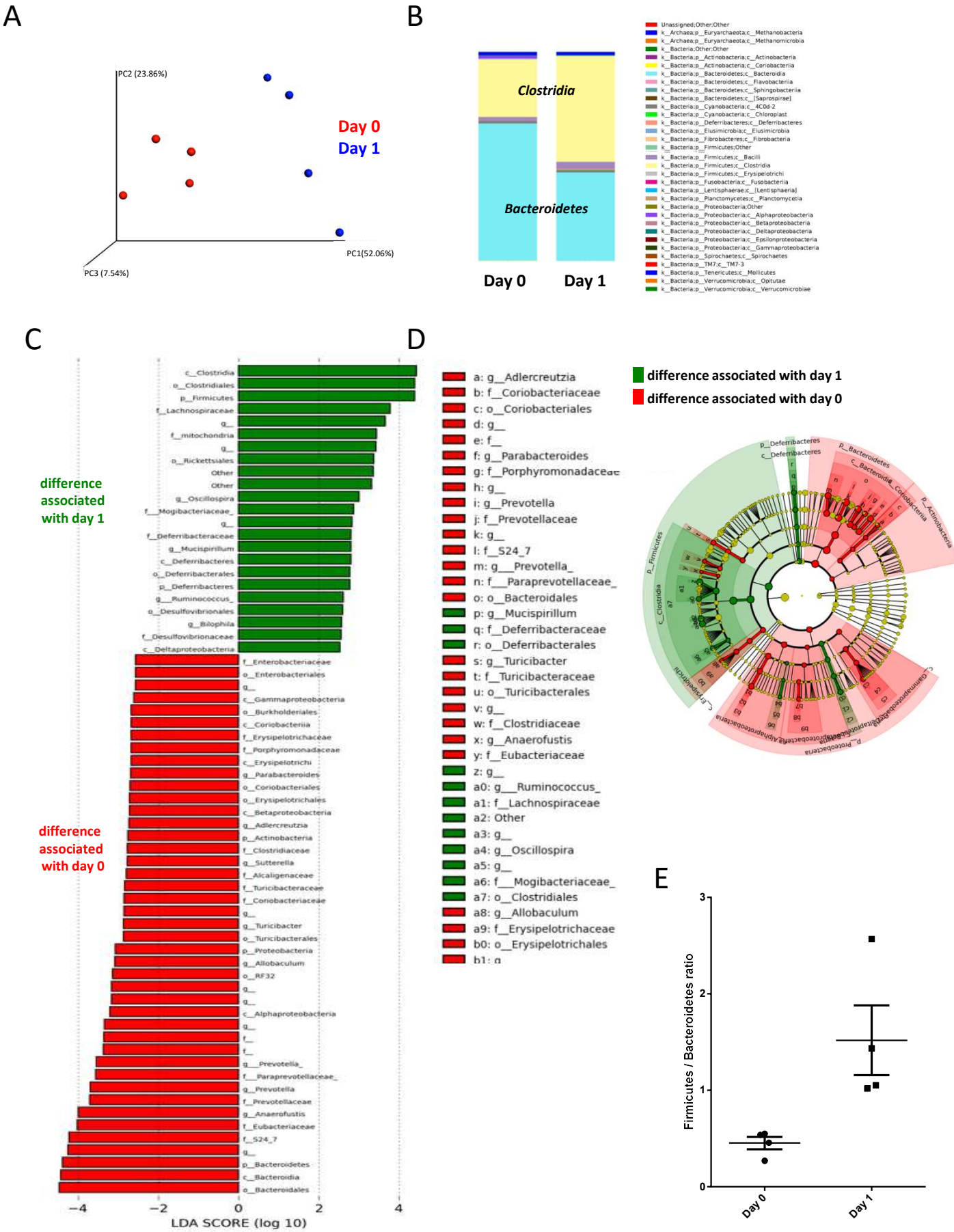
A
PC2 (23.86%)
PC1(52.06%)
PC3 (7.54%)
Day 0
Day 1
B
Clostridia
Bacteroidetes
Day 0
Day 1
C
difference associated with day 1
difference associated with day 0
c__Clostridia
o__Clostridiales
p__Firmicutes
f__Lachnospiraceae
g__
f__mitochondria
g__
o__Rickettsiales
Other
Other
g__Oscillospira
f__Mogibacteriaceae_
g__
f__Deferribacteraceae
g__Mucispirillum
c__Deferribacteres
o__Deferribacterales
p__Deferribacteres
g__Ruminococcus_
o__Desulfovibrionales
g__Bilophila
f__Desulfovibrionaceae
c__Deltaproteobacteria
f__Enterobacteriaceae
o__Enterobacteriales
g__
c__Gammaproteobacteria
o__Burkholderiales
c__Coriobacteriia
f__Erysipelotrichaceae
f__Porphyromonadaceae
c__Erysipelotrichi
g__Parabacteroides
o__Coriobacteriales
o__Erysipelotrichales
c__Betaproteobacteria
g__Adlercreutzia
p__Actinobacteria
f__Clostridiaceae
g__Sutterella
f__Alcaligenaceae
f__Turicibacteraceae
f__Coriobacteriaceae
g__
g__Turicibacter
o__Turicibacterales
p__Proteobacteria
g__Allobaculum
o__RF32
g__
g__
c__Alphaproteobacteria
g__
f__
f__
g__Prevotella_
f__Paraprevotellaceae_
g__Prevotella
f__Prevotellaceae
g__Anaerofustis
f__Eubacteriaceae
f__S24_7
g__
p__Bacteroidetes
c__Bacteroidia
o__Bacteroidales
−4
−2
0
2
4
LDA SCORE (log 10)
D
a: g__Adlercreutzia
b: f__Coriobacteriaceae
c: o__Coriobacteriales
d: g__
e: f__
f: g__Parabacteroides
g: f__Porphyromonadaceae
h: g__
i: g__Prevotella
j: f__Prevotellaceae
k: g__
l: f__S24_7
m: g__Prevotella_
n: f__Paraprevotellaceae_
o: o__Bacteroidales
p: g__Mucispirillum
q: f__Deferribacteraceae
r: o__Deferribacterales
s: g__Turicibacter
t: f__Turicibacteraceae
u: o__Turicibacterales
v: g__
w: f__Clostridiaceae
x: g__Anaerofustis
y: f__Eubacteriaceae
z: g__
a0: g__Ruminococcus_
a1: f__Lachnospiraceae
a2: Other
a3: g__
a4: g__Oscillospira
a5: g__
a6: f__Mogibacteriaceae_
a7: o__Clostridiales
a8: g__Allobaculum
a9: f__Erysipelotrichaceae
b0: o__Erysipelotrichales
b1: g
difference associated with day 1
difference associated with day 0
E
Firmicutes / Bacteroidetes ratio
0
1
2
3
Day 0
Day 1

Figure S2

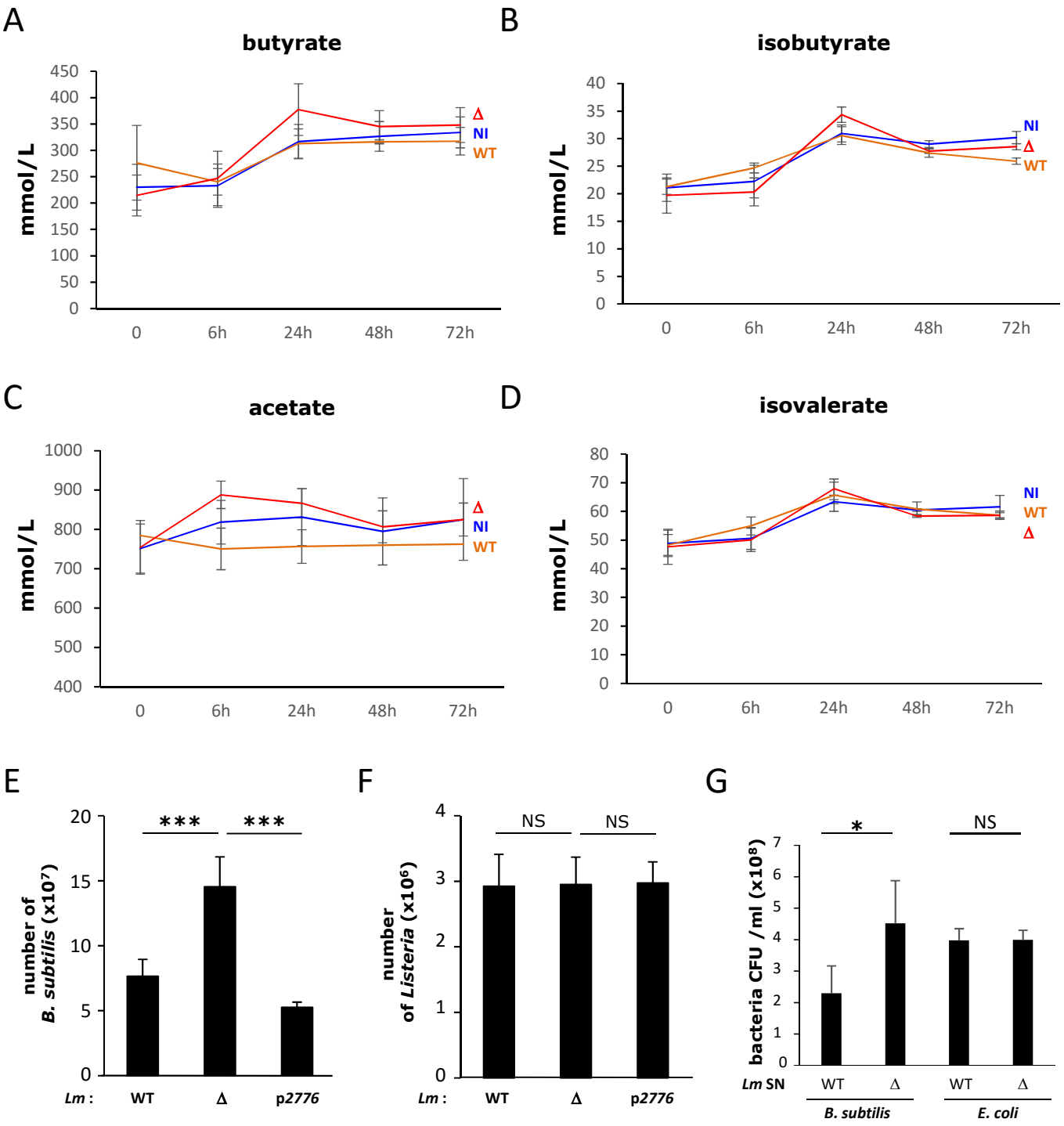
A
butyrate
mmol/L
450
400
350
300
250
200
150
100
50
0
0
6h
24h
48h
72h
Δ
NI
WT
B
isobutyrate
mmol/L
40
35
30
25
20
15
10
5
0
0
6h
24h
48h
72h
NI
Δ
WT
C
acetate
mmol/L
1000
900
800
700
600
500
400
0
6h
24h
48h
72h
Δ
NI
WT
D
isovalerate
mmol/L
80
70
60
50
40
30
20
10
0
0
6h
24h
48h
72h
NI
WT
Δ
E
number of B. subtilis (x10⁷)
20
15
10
5
0
***
***
Lm :
WT
Δ
p2776
F
number of Listeria (x10⁶)
4
3
2
1
0
NS
NS
Lm :
WT
Δ
p2776
G
bacteria CFU /ml (x10⁸)
7
6
5
4
3
2
1
0
*
NS
Lm SN
WT
Δ
WT
Δ
B. subtilis
E. coli

Figure S3

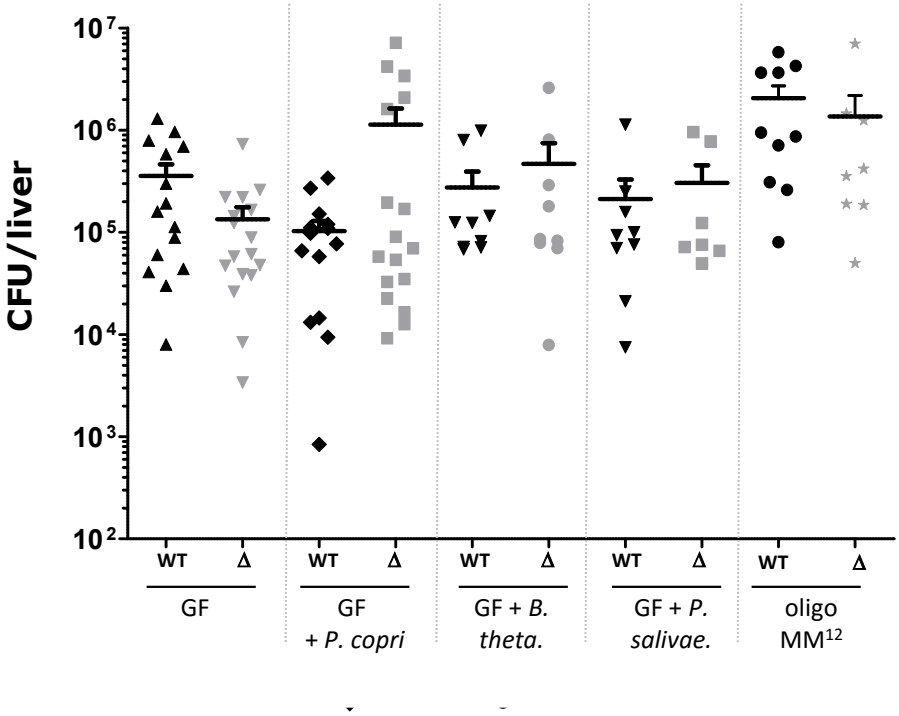
CFU/liver
10^7
10^6
10^5
10^4
10^3
10^2
WT
Δ
GF
GF + *P. copri*
GF + *B. theta.*
GF + *P. salivae.*
oligo MM^{12}

Figure S4

Table S1 Oligonucleotides used in study, related to methods, Figure S1, Figure 2 and Figure 3

Experiment	Primer ID	Sequence	Source
Oligonucleotides used to create deletion mutant	Lmo2776-DelA	GGAAGATCTACATCCTTCACAGGGAAATG	This study
	Lmo2776-DelB	TGTATTCTCCTCTCTTTCAAATTAA	
	Lmo2776-DelC	TTAATTTGAAAGAGAGGAGAATACATTCCTATAAAGCTAAGAAATATTTC	
	Lmo2776-DelD	CGGCCATGGAGCAAAGTCATAAGTAACGGGATAT	
Sequencing insert in pAD-based plasmid	pPL2-Fw	TTCGACCCGGTCGTCGGTTC	Balestrino et al, 2010
	pPL2-Rv	CTTAGACGTCATTAACCCTCAC	
Verification of pAD integration in the *Lm* chromosome	NC16	GTCAAAACATACGCTCTTATC	
	PL95	ACATAATCAGTCCAAAGTAGATGC	
qRT-PCR for gene expression level, related to Figure S1	lmo27741	GTGTTAGAAAACTTATCCATTACAGG	This study
	lmo27742	ATCATCCAAGTTGCCTGTTGGTTCG	
	lmo27751	GGTCTTTAAAGGTTTATGACTTTGG	
	lmo27752	CCCATATACGATTAACTAATAACCG	
	lmo2776 RT1	GTATGTGTTTTAGCGATAGCA	
	lmo2776 RT2	ATAATGTCTATCTTGTCCCC	
	lmo2777 RT1	CTACCACGGAAATGATCGCC	
	lmo2777 RT2	GCACACTAAAGGAGGTAGCG	
	rpoB F	GCGAACATGCAACGTCAAGCAGTA	
	rpoB R	ATGTTTGGCAGTTACAGCAGCACC	
q-PCR for 16S rRNA based bacterial quantification, related to Figure 2 and 3	Prevotella 16S F	CACRGTAAACGATGGATGCC	Scher et al, 2013
	Prevotella 16S R	GGTCGGGTTGCAGACC	
	Universal 16S F	ACTCCTACGGGAGGCAGCAGT	
	Universal 16S R	ATTACCGCGGCTGCTGGC	
	Am_fwd	CAGCACGTGAAGGTGGGGAC	
	Am_rev	CCTTGCGGTTGGCTTCAGAT	